Lenia — Biology of Artificial Life

Bert Wang-Chak Chan*
Hong Kong

Dec 2018

Abstract

We report a new model of artificial life called *Lenia* (from Latin *lenis* "smooth"), a two-dimensional cellular automaton with continuous space-time-state and generalized local rule. Computer simulations show that Lenia supports a great diversity of complex autonomous patterns or "life-forms" bearing resemblance to real-world microscopic organisms. More than 400 species in 18 families have been identified, many discovered via interactive evolutionary computation. They differ from other cellular automata patterns in being geometric, metameric, fuzzy, resilient, adaptive, and rule-generic.

We present basic observations of the model regarding the properties of space-time and basic settings. We provide a board survey of the life-forms, categorize them into a hierarchical taxonomy, and map their distribution in the parameter hyperspace. We describe their morphological structures and behavioral dynamics, propose possible mechanisms of their self-propulsion, self-organization and plasticity. Finally, we discuss how the study of Lenia would be related to biology, artificial life, and artificial intelligence.

Keywords: artificial life; geometric cellular automata; complex system

1 Introduction

Among the long-term goals of *artificial life* are to simulate existing biological life and to create new life forms using artificial systems. These are expressed in the fourteen open problems in artificial life [1], in which number three is of particular interest here:

> *Determine whether fundamentally novel living organizations can exist.*

There have been numerous efforts in creating and studying novel mathematical models that are capable of simulating complex life-like dynamics. Examples

*albert.chak@gmail.com

include particle systems like Swarm Chemistry [2], Primordial Particle Systems (PPS) [3]; reaction-diffusion systems like the U-Skate World [4]; cellular automata like the Game of Life (GoL) [5], elementary cellular automata (ECA) [6]; evolutionary systems like virtual creatures [7], soft robots [8, 9]. These models have a common theme — let there be countless modules or particles and (often localized) interactions among them, a complex system with interesting autonomous patterns will emerge, just like how life emerged on Earth 4.28 billion years ago [10].

Life can be defined as the capabilities of self-organizing (morphogenesis), self-regulating (homeostasis), self-directing (motility), self-replicating (reproduction), entropy reduction (metabolism), growth (development), response to stimuli (sensitivity), response to environment (adaptability), and evolving through mutation and selection (evolvability) (e.g., [11, 12, 13, 14]). Models of artificial life are able to reproduce some of these capabilities with various levels of fidelity. Lenia, the subject of this paper, is able to achieve many of them, except self-replication that is yet to be discovered.

Lenia also captures a few subjective characteristics of life, like vividness, fuzziness, aesthetic appeal, and the great diversity and subtle variety in patterns that a biologist would have the urge to collect and catalogue them. If there is some truth in the biophilia hypothesis [15] that humans are innately attracted to nature, it may not be too far-fetched to suggest that these subjective experiences are not merely feelings but among the essences of life as we know it.

The diverse life in Lenia, although being interesting, should not be treated as a mere curiosity. As shown in this paper, this form of artificial life might be deeply linked to biological life in surprising ways, like metamerism / multicellularity, symmetry, plasticity, and common issues like the species problem. They warrant scientific investigations.

Due to similarities between life on Earth and Lenia, we borrow terminologies and concepts from biology, like taxonomy (corresponds to categorization), binomial nomenclature (naming), ecology (parameter space), morphology (structures), behavior (dynamics), physiology (mechanisms), and allometry (statistics). We also borrow space-time (grid and time-step) and fundamental laws (local rule) from physics. With a few caveats, these borrowings are useful in providing more intuitive characterization of the system, and may facilitate discussions on how Lenia or similar models could give answers to life [16], the universe [17], and everything.

1.1 Background

A *cellular automaton* (CA, plural: cellular automata) is a mathematical model where a grid of sites, each having a particular state at a moment, are being updated repeatedly according to each site's neighboring sites and a local rule. Since its conception by John von Neumann and Stanislaw Ulam [18, 19], various CAs have been invented and investigated, the most famous being Stephen Wolfram's one-dimensional elementary cellular automata (ECA) [6, 17] and John H. Conway's two-dimensional *Game of Life* (GoL) [5, 20].

Model	Type	Space	Neighborhood	N. sum	Growth	Update	Time	State
ECA, GoL	CA	unary	nearest cube	totalistic	intervals	replace	unary	unary
Primordia	CA	unary	nearest cube	totalistic	intervals	replace	unary	extended
LtL	GCA	fractional	extended cube	totalistic	intervals	replace	unary	unary
RealLife	EA	continuous	continuous cube	totalistic	intervals	replace	unary	unary
SmoothLife	GCA	fractional	extended shell	totalistic	intervals	increment	fractional [3]	fractional
Cont. GoL	EA	continuous	continuous ball	totalistic	mapping	replace	unary	continuous
Lenia (disc.)	GCA	fractional	extended ball	weighted	mapping	increment	fractional	fractional
Lenia (cont.)	EA	continuous	continuous ball	weighted	mapping	increment	continuous	continuous

Table 1: Comparison of genericity and continuity in various CAs. Continuous CAs (RealLife, continuous GoL, continuous Lenia) are hypothetical constructs, while others can be simulated in a computer. (GCA = geometrical cellular automata, EA = Euclidean automata, see "Discussion")

GoL is the starting point of where Lenia came from. GoL consists of a two-dimensional square grid, 2-state sites, 8-site neighborhood, and a totalistic update rule with survival/birth intervals {2, 3} and {3}. It produces a whole universe of interesting patterns [21] ranging from simple "still lifes", "oscillators" and "spaceships", to complex constructs like pattern emitters, self-replicators, logic gates, and even fully operational computers thanks to its Turing completeness [22].

1.1.1 Evolution of generalization

Several aspects of GoL can be generalized via the following path:

discrete (unary → extended → fractional) → continuous

A *unary* property (e.g. dead-or-alive state) can be *extended* into a range (multi-state), which is equivalent to a *fractional* property by being normalized into the unit range, and becomes *continuous* by further splitting the range into infinitesimals (real number state). The local rule can be generalized from the basic ECA/GoL style (totalistic sum, survival/birth intervals, replacing update) to smooth parameterized operations (weighted sum, growth mapping, incremental update).

By comparing various CAs including ECA, GoL, continuous GoL [23], Larger-than-Life (LtL) [24, 25, 26], RealLife [27], SmoothLife[1] [28], Primordia[2], and Lenia, we observe the *evolution of generalization* with increasing genericity and continuity (Table 1, Figure 1). This suggests that Lenia is currently at the latest stage of generalizing GoL, although there may be room for further generalizations.

[1] SmoothLife and Lenia, being independent developments, exhibit striking resemblance in model and generated patterns. This can be considered an instance of "convergent evolution" in generalizing GoL.

[2] Primordia is a precursor to Lenia, written in JavaScript/HTML by the author circa 2005. It had multi-states and extended survival/birth intervals, with automatic pattern detection.

[3] Fractional time in SmoothLife was suggested in the paper and achieved in computer implementations.

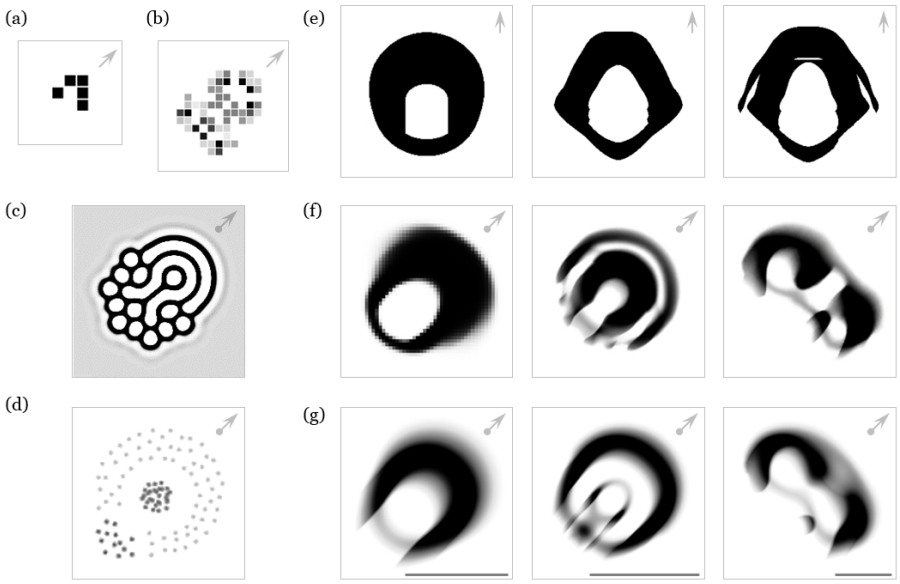

Figure 1: Patterns in artificial life models: cellular automata (a-b, e-g), reaction-diffusion (b) and particle swarm (c). (↑= orthogonal; ↗= diagonal; ⬈= omni-directional; scale bar is unit length = kernel radius). **(a)** Game of Life (GoL): "glider". **(b)** Primordia: "DX:8/762". **(c)** U-Skate World: "Jellyfish" [29]. **(d)** Swarm Chemistry: "Fast Walker & Slow Follower" [30]. **(e)** Larger-than-Life (LtL): "bug with stomach" using ball neighborhood, "bug with ribbed stomach", "bug with wings" [26]. **(f)** SmoothLife: "smooth glider", "pulsating glider", "wobbly glider" [28, 31, 32]. **(g)** Lenia: *Scutium*, *Kronium*, *Pyroscutium*.

2 METHODS

We describe the methods of constructing and studying Lenia, including its mathematical definition, *in silico* simulation, strategies of evolving new lifeforms, and how to perform observational and statistical analysis.

2.1 Definitions

Mathematically, a CA is defined by a 5-tuple[4] $\mathcal{A} = (\mathcal{L}, \mathcal{T}, \mathcal{S}, \mathcal{N}, \phi)$, where $\mathcal{L}$ is the d-dimensional *lattice* or *grid*, $\mathcal{T}$ is the *timeline*, $\mathcal{S}$ is the *state set*, $\mathcal{NL}$ is the *neighborhood* (of the origin), $\phi : \mathcal{S}^{\mathcal{N}} \to \mathcal{S}$ is the *local rule*.

Define $\mathbf{A}^t : \mathcal{L} \to \mathcal{S}$ as the *configuration* or *pattern* (i.e. collection of states over the whole grid) at time $t \in \mathcal{T}$. $\mathbf{A}^t(\mathbf{x})$ is the state of site $x \in \mathcal{L}$, and $\mathbf{A}^t(\mathcal{N}_\mathbf{x}) = \{\mathbf{A}^t(\mathbf{n}) : \mathbf{n} \in \mathcal{N}_\mathbf{x}\}$ is the state collection over the sites neighbor-

[4]Conventionally a CA is defined by a 4-tuple $\mathcal{A} = (\mathcal{L}, \mathcal{S}, \mathcal{N}, \phi)$, here the timeline $\mathcal{T}$ is added to indicate its variability.

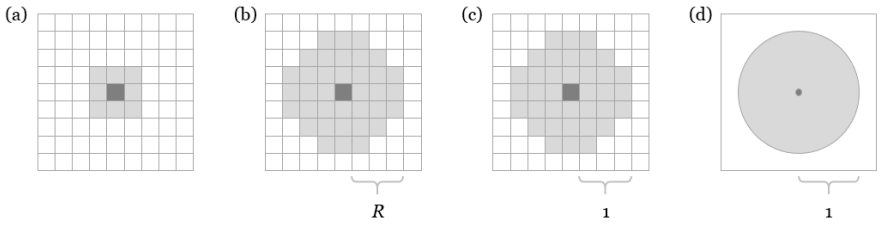

Figure 2: Neighborhoods in various CAs. **(a)** 8-site Moore neighborhood in GoL. **(b-d)** Neighborhoods in Lenia, including range R extended neighborhood (b) and its normalization (c) in discrete Lenia, and the unit ball neighborhood in continuous Lenia (d).

hood $\mathcal{N}_{\mathbf{x}} = \{\mathbf{x} + \mathbf{n} : \mathbf{n} \in \mathcal{N}\}$. The global rule is $\Phi : \mathcal{S}^{\mathcal{L}} \to \mathcal{S}^{\mathcal{L}}$ such that $\Phi(\mathbf{A})(\mathbf{x}) = \phi(\mathbf{A}(\mathcal{N}_{\mathbf{x}}))$. Starting from an initial configuration $\mathbf{A}^0$, the grid is updated according to the global rule ϕ for each time-step Δt, leading to the following time-evolution:

$$\Phi(\mathbf{A}^0) = \mathbf{A}^{\Delta t}, \Phi(\mathbf{A}^{\Delta t}) = \mathbf{A}^{2\Delta t}, \ldots, \Phi(\mathbf{A}^t) = \mathbf{A}^{t+\Delta t}, \ldots \tag{1}$$

After N repeated updates (or *generations*):

$$\Phi^N(\mathbf{A}^t) = \mathbf{A}^{t+N\Delta t} \tag{2}$$

2.1.1 Definition of Game of Life

Take GoL as an example, $\mathcal{A}_{\text{GoL}} = (\mathcal{L}, \mathcal{T}, \mathcal{S}, \mathcal{N}, \phi)$, where $\mathcal{L} = \mathbb{Z}^2$ is the two-dimensional discrete grid; $\mathcal{T} = \mathbb{Z}$ is the discrete timeline; $\mathcal{S} = \{0, 1\}$ is the unary state set; $\mathcal{N} = \{-1, 0, 1\}^2$ is the Moore neighborhood (Chebyshev L^∞ norm) including the site itself and its 8 neighbors (Figure 2(a)).

The totalistic neighborhood sum of site x is:

$$\mathbf{S}^t(\mathbf{x}) = \sum_{n \in \mathcal{N}} \mathbf{A}^t(\mathbf{x} + \mathbf{n}) \tag{3}$$

Every site is updated synchronously according to the local rule:

$$\mathbf{A}^{t+1}(\mathbf{x}) = \begin{cases} 1 & \text{if } \mathbf{A}^t(\mathbf{x}) = 0 \text{ and } \mathbf{S}^t(\mathbf{x}) \in \{3\} \ \textit{(birth)} \\ 1 & \text{if } \mathbf{A}^t(\mathbf{x}) = 1 \text{ and } \mathbf{S}^t(\mathbf{x}) \in \{3, 4\} \ \textit{(survival)} \\ 0 & \text{otherwise } \textit{(death)} \end{cases} \tag{4}$$

2.1.2 Definition of Lenia

Discrete Lenia (DL) generalizes GoL by extending and then normalizing the space-time-state dimensions. DL is used for computer simulation and analysis, and with normalization, patterns from different dimensions can be compared.

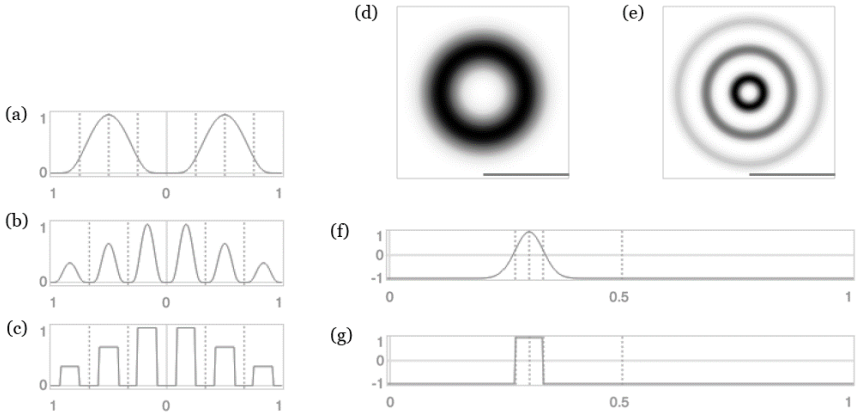

Figure 3: Core functions in Lenia. **(a-c)** Cross-section of the kernel: kernel core $K_C(r)$ using exponential function (a), and kernel shell $K_S(r;\beta)$ with peaks $\beta = (1, 2/3, 1/3)$ using exponential (b) or rectangular core function (c). **(d-e)** Kernel core (d) and kernel shell (e) as displayed in the grid, showing the "influence" (convolution weight) of the site on its neighborhood (darker = larger weight, more influence). **(f-g)** Growth mapping $G(u;\mu,\sigma)$ with $\mu = 0.3, \sigma = 0.03$ using exponential (f) or rectangular (g) function.

Continuous Lenia (CL) is hypothesized to exist by taking the dimensions of DL to their continuum limits.

The state set is extended to $\mathcal{S} = \{0, 1, 2, \ldots, P\}$ with maximum $P \in \mathbb{Z}$. The neighborhood is extended to a discrete ball (Euclidean L^2 norm) of range $R \in \mathbb{Z}$ that $\mathcal{N} = \mathbb{B}_R[0] = \{\mathbf{x} \in \mathcal{L} : \|x\|_2 \leq R\}$ (Figure 2(b)).

To normalize, define or redefine $R, T, P \in \mathbb{Z}$ as the *space resolution*, *time resolution*, and *state resolution*, and their reciprocals $\Delta x = 1/R, \Delta t = 1/T, \Delta p = 1/P$ as the *site distance*, *time step* (fractional), and *state precision*, respectively. The space-time-state dimensions are scaled by the reciprocals, so that

$$\mathcal{L} = \Delta x\, \mathbb{Z}^2, \quad \mathcal{T} = \Delta t\, \mathbb{Z}, \quad \mathcal{S} = \Delta p\, \{0 \ldots P\} \tag{5}$$

and the neighborhood is normalized to become a discrete unit ball $\mathcal{N} = \mathbb{B}_1[0]$. (Figure 2(c)) As the resolutions approach infinity $R \to \infty, T \to \infty, P \to \infty$ and the differences $\Delta x, \Delta t, \Delta p$ become infinitesimals $\mathrm{d}x, \mathrm{d}t, \mathrm{d}p$, it is conjectured that the space-time-state dimensions will approach their continuum limits, i.e. the Euclidean space, the real timeline, and real number states of the unit interval

$$\mathcal{L} = \mathbb{R}^2, \quad \mathcal{T} = \mathbb{R}, \quad \mathcal{S} = [0, 1] \tag{6}$$

and the neighborhood will approach the continuous unit ball $\mathcal{N} = \mathbb{B}_1[0]$. (Figure 2(d))

However, there is a cardinality leap between the discrete dimensions in DL and the continuous dimensions in CL. The existence of the space continuum

limit was proved mathematically in [27], and our computer simulations provide empirical evidence for continuum limit of space and time (see "Physics" section). Further rigorous proofs are needed.

2.1.3 Local rule

To apply Lenia's local rule to every site x at time t, the *potential distribution* $\mathbf{U}^t$ is calculated by convolution of its neighborhood with a *kernel* $\mathbf{K} : \mathcal{N} \to \mathcal{S}$:

$$\mathbf{U}^t(\mathbf{x}) = \mathbf{K} * \mathbf{A}^t(\mathbf{x}) = \sum_{n \in \mathcal{N}} \mathbf{K}(\mathbf{n}) \mathbf{A}^t(\mathbf{x}+\mathbf{n}) \; \Delta x^2 \qquad \text{in DL}$$
$$\int_{n \in \mathcal{N}} \mathbf{K}(\mathbf{n}) \mathbf{A}^t(\mathbf{x}+\mathbf{n}) \; \mathrm{d}x^2 \qquad \text{in CL} \tag{7}$$

Feeding the potential into the *growth mapping* $G : [0,1] \to [-1,1]$ yields the *growth distribution* $\mathbf{G}^t$

$$\mathbf{G}^t(\mathbf{x}) = G(\mathbf{U}^t(\mathbf{x})) \tag{8}$$

Every state is updated by adding a small fraction Δt of the growth and clipped back to the unit interval $[0,1]$, and the time is now $t + \Delta t$. (In CL, the time step Δt is replaced by infinitesimal $\mathrm{d}t$)

$$\begin{aligned} \mathbf{A}^{t+\Delta t}(\mathbf{x}) &= \left[\mathbf{A}^t(\mathbf{x}) + \Delta t \; \mathbf{G}^t(\mathbf{x})\right]_0^1 \\ &= \left[\mathbf{A}^t(\mathbf{x}) + \Delta t \; G(\mathbf{K} * \mathbf{A}^t(\mathbf{x}))\right]_0^1 \end{aligned} \tag{9}$$

where $[n]_a^b = \min(\max(n, a), b)$ is the clip function.

2.1.4 Kernel

The kernel $\mathbf{K}$ is constructed by *kernel core* $K_C : [0,1] \to [0,1]$ which determines the inner "texture" of the kernel, *kernel shell* $K_S : [0,1] \to [0,1]$ which determines its "skeleton", and normalization which makes sure $\mathbf{K} * \mathbf{A} \in [0,1]$. The convolution with kernel (i.e. weighted sum) is a generalization of the totalistic sum in GoL.

The kernel core K_C is any unimodal function satisfying $K_C(0) = K_C(1) = 0$ and usually $K_C(1/2) = 1$. By taking polar distance as argument, it creates a uniform ring around the site (Figure 3(a, d)). The function can be exponential, polynomial, trigonometric, trapezoidal, or rectangular, etc. (Figure 3(a-c)); the exponential kernel core is used throughout this paper.

$$K_C(r) = \begin{cases} \exp\left(\alpha - \dfrac{\alpha}{4r(1-r)}\right) & \text{exponential, } \alpha = 4 \\ (4r(1-r))^{\alpha} & \text{polynomial, } \alpha = 4 \\ \Pi_{1/4,3/4}(r) & \text{rectangular} \\ \dots \end{cases} \tag{10}$$

The kernel shell K_S takes a vector parameter $\beta = (\beta_1, \beta_2, \ldots, \beta_B) \in [0,1]^B$ (*kernel peaks*) of size B (*the rank*) and copies the kernel core into concentric rings of equal thickness with peak heights β_i (Figure 3(b, e)).

$$K_S(r;\beta) = \beta_{\lfloor Br \rfloor} K_C(Br \bmod 1) \tag{11}$$

Finally, the kernel is normalized:

$$\mathbf{K}(\mathbf{n}) = \frac{K_S(\|\mathbf{n}\|_2)}{|K_S|} \tag{12}$$

where $|K_S| = \sum_{\mathcal{N}} K_S \, \Delta x^2$ in DL, or $\int_{\mathcal{N}} K_S \, \mathrm{d}x^2$ in CL.

Notes on parameter β:

- A vector β of rank B is equivalent to an extended vector with n trailing zeros while space resolution R is scaled by factor $(B+n)/B$, e.g. $\beta = (1) \equiv (1,0,0)$ with R scaled by 3.
- A vector β where $\forall i \ \beta_i \neq 1$ is equivalent to a scaled vector $\beta / \max(\beta_i)$ where $\exists i \ \beta_i = 1$ while the kernel is unchanged due to normalization, e.g. $\beta = (1/3, 0, 2/3) \equiv (1/2, 0, 1)$.
- Consequently, all possible β of rank B as a B-dimensional hypercube can be projected onto its $(B-1)$-dimensional hypersurfaces where $\exists i \ \beta_i = 1$. (see Figure 10 for $B = 3$)

2.1.5 Growth mapping

The growth mapping $G : [0,1] \to [-1,1]$ is any unimodal, nonmonotonic function with parameters $\mu, \sigma \in \mathbb{R}$ (*growth center* and *growth width*) satisfying $G(\mu) = 1$, and σ roughly corresponds to the width of its peak (cf. $\zeta(\cdot)$ in [23]). The function can be exponential, polynomial, trigonometric, trapezoidal, or rectangular, etc. (Figure 3(f-g)); the exponential growth mapping is used throughout this paper.

$$G(u;\mu,\sigma) = \begin{cases} 2\exp\left(-\dfrac{(u-\mu)^2}{2\sigma^2}\right)^{\alpha} - 1 & \text{exponential} \\ 2\left(1 - \dfrac{(u-\mu)^2}{9\sigma^2}\right)^{\alpha} - 1 & \text{polynomial, } \alpha = 4 \\ 2\Pi_{\mu-\sigma,\mu+\sigma}(u) - 1 & \text{rectangular} \\ \ldots \end{cases} \tag{13}$$

The growth mapping is a generalization of the survival/birth intervals in GoL, where the positive, near zeros, and negative values correspond to the birth, survival, and death intervals, respectively.

2.1.6 GoL inside Lenia

GoL can be considered a special case of discrete Lenia with $R = T = P = 1$, using a variant of the rectangular kernel core:

$$K_C(r) = \begin{cases} 1 & \text{if } 1/2 < r \leq 3/2 \\ 1/2 & \text{if } r \leq 1/2 \\ 0 & \text{otherwise} \end{cases} \tag{14}$$

and the rectangular growth mapping with $\mu = 0.35, \sigma = 0.07$.

2.1.7 Summary

In summary, discrete and continuous Lenia are defined as:

$$\begin{aligned} \mathcal{A}_{\text{DL}} = \big(&\Delta x\, \mathbb{Z}^2, \Delta t\, \mathbb{Z}, \Delta p\, \{0 \dots P\}, \mathbb{B}_1[0], \\ &\mathbf{A}^{t+\Delta t} \mapsto \left[\mathbf{A}^t + \Delta t\, G_{\mu,\sigma}(\mathbf{K}_\beta * \mathbf{A}^t)\right]_0^1\big) \end{aligned} \tag{15}$$

$$\begin{aligned} \mathcal{A}_{\text{CL}} = \big(&\mathbb{R}^2, \mathbb{R}, [0,1], \mathbb{B}_1[0], \\ &\mathbf{A}^{t+\mathrm{d}t} \mapsto \left[\mathbf{A}^t + \mathrm{d}t\, G_{\mu,\sigma}(\mathbf{K}_\beta * \mathbf{A}^t)\right]_0^1\big) \end{aligned} \tag{16}$$

The associated dimensions are: space-time-state resolutions R, T, P, differences $\Delta x, \Delta t, \Delta p$, infinitesimals $\mathrm{d}x, \mathrm{d}t, \mathrm{d}p$. The associated parameters are: growth center μ, growth width σ, kernel peaks β of rank B. The mutable core functions are: kernel core K_C, growth mapping G.

2.2 Computer Implementation

Discrete Lenia (DL) can be implemented with the pseudocode below, assuming an array programming language is used (e.g. Python with NumPy, MATLAB, Wolfram).

Interactive programs have been written in JavaScript / HTML5, Python, and MATLAB to provide user interface for new species discovery (Figure 4(a-b)). Non-interactive program has been written in C#.NET for automatic traverse through the parameter space using a flood fill algorithm (breath-first or depth-first search), providing species distribution, statistical data and occasionally new species.

State precision Δp can be implicitly implemented as the precision of floating-point numbers. For values in the unit interval $[0, 1]$, the precision ranges from 2^{-126} to 2^{-23} (about 1.2×10^{-38} to 1.2×10^{-7}) using 32-bit single-precision, or from 2^{-1022} to 2^{-52} (about 2.2×10^{-308} to 2.2×10^{-16}) using 64-bit double-precision [33]. That means $P > 10^{15}$ using double precision.

Discrete convolution can be calculated as the sum of element-wise products:

$$\mathbf{K} * \mathbf{A}^t(\mathbf{x}) = \sum_{\mathbf{n} \in \mathcal{N}} \mathbf{K}(\mathbf{n}) \mathbf{A}^t(\mathbf{x} + \mathbf{n}) \tag{17}$$

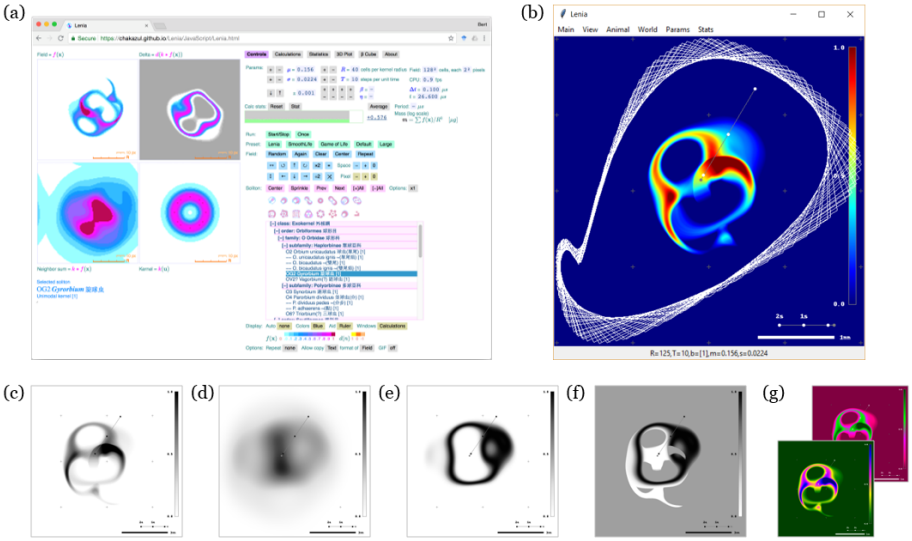

Figure 4: Computer implementations of Lenia with interactive user interfaces. **(a-b)** Web version run in Chrome browser (a) and Python version with GPU support (b). **(c-f)** Different views during simulation, including the configuration At (c), the potential Ut (d), the growth Gt (e), and the actual change $\Delta \mathbf{A}/\Delta t = (\mathbf{A}^{t+\Delta t} - \mathbf{A}^t)/\Delta t$ (f). **(g)** Other color schemes.

or alternatively, using discrete Fourier transform (DFT) according to the convolution theorem:

$$\mathbf{K} * \mathbf{A}^t = \mathcal{F}^{-1}\left\{\mathcal{F}\{\mathbf{K}\} \cdot \mathcal{F}\{\mathbf{A}^t\}\right\} \tag{18}$$

Efficient calculation can be achieved using fast Fourier transform (FFT) [34], pre-calculation of the kernel's FFT $\mathcal{F}\{\mathbf{K}\}$, and parallel computing like GPU acceleration. The DFT/FFT approach automatically produces a periodic boundary condition.

2.2.1 Pseudocode

Symbol `@` indicates the data type of two-dimensional matrix of floating-point numbers.

```
function pre_calculate_kernel(beta, dx)
  @radius = get_polar_radius_matrix(SIZE_X, SIZE_Y) * dx
  @Br = size(beta) * @radius
  @kernel_shell = beta[floor(@Br)] * kernel_core(@Br % 1)
  @kernel = @kernel_shell / sum(@kernel_shell)
  @kernel_FFT = FFT_2D(@kernel)
  return @kernel, @kernel_FFT
end

function run_automaton(@world, @kernel, @kernel_FFT, mu, sigma, dt)
```

```
  if size(@world) is small
    @potential = elementwise_convolution(@kernel, @world)
  else
    @world_FFT = FFT_2D(@world)
    @potential_FFT = elementwise_multiply(@kernel_FFT, @world_FFT)
    @potential = FFT_shift(real_part(inverse_FFT_2D(@potential_FFT)))
  end
  @growth = growth_mapping(@potential, mu, sigma)
  @new_world = clip(@world + dt * @growth, 0, 1)
  return @new_world, @growth, @potential
end

function simulation()
  R, T, mu, sigma, beta = get_parameters()
  dx = 1/R;  dt = 1/T;  time = 0
  @kernel, @kernel_FFT = pre_calculate_kernel(beta, dx)
  @world = get_initial_configuration(SIZE_X, SIZE_Y)
  repeat
    @world, @growth, @potential = run_automaton(@world,
        @kernel, @kernel_FFT, mu, sigma, dt)
    time = time + dt
    display(@world, @potential, @growth)
  end
end
```

2.2.2 User interface

For implementations requiring an interactive user interface, one or more of the following components are recommended:

- Controls for starting and stopping CA simulation
- Panels for displaying different stages of CA calculation
- Controls for changing parameters and space-time-state resolutions
- Controls for randomizing, transforming and editing the current configuration
- Controls for saving, loading, and copy-and-pasting configurations
- Clickable list for loading predefined patterns
- Utilities for capturing the display output (e.g. static or animated image, movie clip)
- Controls for customizing the layout (e.g. grid size, color map)
- Controls for auto-centering, auto-rotating and temporal sampling
- Panels or overlays for displaying real-time statistical analysis

2.2.3 Pattern storage

A pattern can be stored for publication and sharing using a data exchange format (e.g. JSON, XML) that includes the *run-length encoding* (RLE) of the two-dimensional array At and its associated parameters $(R, T, P, \mu, \sigma, \beta, K_C, G)$, or alternatively, using a plaintext format (e.g. CSV) for further analysis or manipulation in numeric software.

A long list of interesting patterns can be saved in a JSON/XML list for program retrieval. To save storage space, patterns can be stored with space

resolution R as small as possible (usually $10 \leq R \leq 20$) thanks to Lenia's scale invariance (see "Physics" section) and re-enlarged upon retrieval.

2.2.4 Environment

Most of computer simulations, experiments, statistical analysis, image and video capturing for this paper were done using the following environments and settings:

- Hardware: Apple MacBook Pro (OS X Yosemite), Lenovo ThinkPad X280 (Microsoft Windows 10 Pro)
- Software: Python 3.7.0, MathWorks MATLAB Home R2017b, Google Chrome browser, Microsoft Excel 2016
- State precision: double precision
- Kernel core and growth mapping: exponential

2.3 Evolving New Species

A self-organizing, autonomous pattern in Lenia is called a *lifeform*, and a kind of similar lifeforms is called a species. Up to the moment, more than 400 species have been discovered. *Interactive evolutionary computation* (IEC) [35] is the major force behind the generation, identification and selection of new species. In evolutionary computation (EC), the fitness function is usually well known and can be readily calculated. However, in the case of Lenia, due to the non-trivial task of pattern recognition, as well as aesthetic factors, evolution of new species often requires human interaction.

Interactive computer programs provide user interface and utilities for human users to carry out mutation and selection operators manually. Mutation operators include parameter tweaking and configuration manipulation. Selection operators include observation via different views for fitness estimation (Figure 3(c-f)) and storage of promising patterns. Selection criteria include survival, long-term stability, aesthetic appeal, and novelty.

Listed below are a few evolutionary strategies learnt from experimenting and practicing.

2.3.1 Random generation

Initial configurations with random patches of non-zero sites were generated and put into simulation using interactive program. This is repeated using different random distributions and different parameters. Given enough time, naturally occurring lifeforms would emerge from the primordial soup, for example *Orbium*, *Scutium*, *Paraptera*, and radial symmetric patterns. (Figure 5(a))

2.3.2 Parameter tweaking

Using an existing lifeform, parameters were changed progressively or abruptly, forcing the lifeform to die out (explode or evaporate) or survive by changing

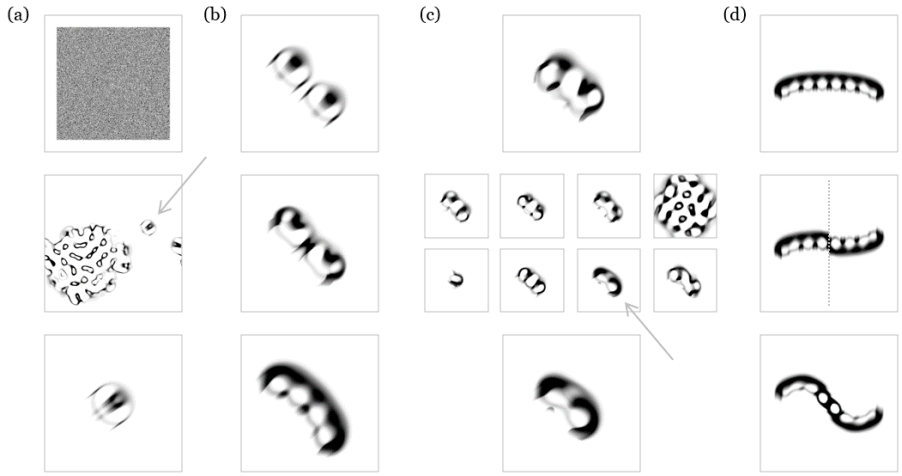

Figure 5: Strategies of evolving new Lenia lifeforms using Interactive Evolutionary Computation (IEC). **(a)** Random generation: random initial configuration is generated (top) and simulation is run (middle), where new lifeforms were spotted (arrow) and isolated (bottom). **(b)** Parameter tweaking: with an existing lifeform (top), parameters are adjusted so that new morphologies or behaviors are observed (middle, bottom). **(c)** Automatic exploration: a starting lifeform (top) is put into an automatic program to explore wide ranges of parameters (middle), where new lifeforms were occasionally discovered (arrow) and isolated (bottom). **(d)** Manual mutation: an existing lifeform (top) is modified, here single-side flipped (middle), and parameter tweaked to stabilize into a new species (bottom).

slightly or morphing into another species. Any undiscovered species with novel structure or behavior were recorded. (Figure 5(b))

Transient patterns captured during random generation could also be stabilized into new species in this way.

Long-chain lifeforms (e.g. Pterifera) could first be elongated by temporary increasing the growth rate (decrease μ or increase σ), then stabilized into new species by reversing growth. Shortening could be done in the opposite manner.

2.3.3 Automatic exploration

Starting from an existing lifeform, automatic program was used to traverse the parameter space (i.e. continuous parameter tweaking). All survived patterns were recorded, among them new species were occasionally found. Currently, automated exploration is ineffective without the aid of artificial intelligence (e.g. pattern recognition), and has only been used for simple conditions (rank 1, mutation by parameter tweaking, selection by survival). (Figure 5(c))

2.3.4 Manual mutation

Patterns were edited or manipulated (e.g. enlarging, shrinking, mirroring, single-side flipping, recombining) using our interactive program or other numeric software, and then parameter tweaked in attempt to stabilize into new species. (Figure 5(d))

2.4 Analysis of Lifeforms

2.4.1 Qualitative analysis

By using computer simulation and visualization and taking advantage of human's innate ability of spatial and temporal pattern recognition, the physical appearances and movements of known species were being observed, documented and categorized, as reported in the "Morphology" and "Behavior" sections. Using automatic traverse program, the distributions of selected species in the parameter space were charted, as reported in the "Ecology" section. A set of criteria, based on the observed similarities and differences among the known species, were devised to categorize them into a hierarchical taxonomy, as reported in the "Taxonomy" section.

2.4.2 Quantitative analysis

Statistical methods were used to analyze lifeforms to compensate limitations in human observation regarding subtle variations and long-term trends. A number of *statistical measures* were calculated over the configuration (i.e. mass distribution) $\mathbf{A}$ and the positive-growth distribution $\mathbf{G}|_{\mathbf{G}>0}$

- *Mass* is the sum of states, $m = \int \mathbf{A}(\mathbf{x})\mathrm{d}\mathbf{x}$ [mg]
- *Volume* is the number of positive states, $V_m = \int_{\mathbf{A}>0} \mathrm{d}\mathbf{x}$ [mm^2]
- *Density* is the density of states, $\rho_m = m/V_m$ [mg mm^{-2}]
- *Growth* is the sum of positive growth, $g = \int_{\mathbf{G}>0} \mathbf{G}(\mathbf{x})\mathrm{d}\mathbf{x}$ [mg s^{-1}]
- *Centroid* is the center of states, $\bar{\mathbf{x}}_m = \int \mathbf{x}\mathbf{A}(\mathbf{x})\mathrm{d}\mathbf{x}/m$
- *Growth center* is the center of positive growth, $\bar{\mathbf{x}}_g = \int_{\mathbf{G}>0} \mathbf{x}\mathbf{G}(\mathbf{x})\mathrm{d}\mathbf{x}/g$
- *Growth-centroid distance* is the distance between the two centers, $d_{gm} = |\bar{\mathbf{x}}_g - \bar{\mathbf{x}}_m|$ [mm]
- *Linear speed* is the linear moving rate of the centroid, $s_m = |\mathrm{d}\bar{\mathbf{x}}_m/\mathrm{d}t|$ [mm s^{-1}]
- *Angular speed* is the angular moving rate of the centroid, $\omega_m = \mathrm{d}/\mathrm{d}t \arg(\mathrm{d}\bar{\mathbf{x}}_m/\mathrm{d}t)$ [rad s^{-1}]
- *Mass asymmetry* is the mass difference across the directional vector, $m_\Delta = \int_{c>0} \mathbf{A}(\mathbf{x})\mathrm{d}\mathbf{x} - \int_{c<0} \mathbf{A}(\mathbf{x})\mathrm{d}\mathbf{x}$ [mg] where $c = \mathrm{d}\bar{\mathbf{x}}_m \times (\mathbf{x} - \bar{\mathbf{x}}_m)$
- *Angular mass* is the second moment of mass from the centroid, $I_m = \int \mathbf{A}(\mathbf{x})(\mathbf{x} - \bar{\mathbf{x}}_m)^2\mathrm{d}\mathbf{x}$ [mg mm^2]
- *Gyradius* is the root-mean-square of site distances from the centroid, $r_m = \sqrt{I_m/m}$ [mm]
- Others e.g. Hu's and Flusser's moment invariants ϕ_i [36, 37]

Note: SI units in microscopic scale were borrowed as units of measure, e.g. "mm" for length, "rad" for angle, "s" for time, "mg" for states (cf. "lu" and "tu" in [4]).

Based on multivariate time-series of statistical measures over a predefined time period, the following "meta-measures" were calculated:

- Summary statistics (mean, median, standard deviation, minimum, maximum, quartiles)
- Quasi-period (estimated using e.g. autocorrelation, periodogram)
- Degree of chaos (e.g. Lyapunov exponent, attractor dimension)
- Probability of survival

The following charts were plotted using various parameters, measures and meta-measures:

- Time series chart (measure vs. time)
- Phase space trajectory (measure vs. measure) (e.g. Figure 17 insets)
- Measure chart (meta vs. meta) (e.g. Figure 14, 16)
- Cross-sectional chart (meta vs. parameter) (e.g. Figure 17)
- μ-σ map (parameter μ vs. σ; information as color) (e.g. Figure 9, 15)
- β-cube (parameter β components as axes; information as color) (e.g. Figure 10)

Over 1.2 billion measures were collected using automatic traverse program and analyzed using numeric software like Microsoft Excel. Results are presented in the "Physiology" section.

2.4.3 Spatiotemporal analysis

Constant motions like translation, rotation and oscillation render visual observation difficult. It is desirable to separate the spatial and temporal aspects of a moving pattern so as to directly assess the static form and estimate the motion frequencies (or quasi-periods).

Linear motion can be removed by *auto-centering*, to display the pattern centered at its centroid $\bar{\mathbf{x}}_m$.

Using *temporal sampling*, the simulation is displayed one frame per N time-steps. When any rotation is perceived as near stationary, the rotation frequency is approximately the display frequency $f_r \approx f_d = 1/(N\Delta t)$. Calculate the sampled angular speed $\omega_s = \theta f_r = 2\pi f_r/n$ where n is the number of radial symmetric axes. Angular motion can be removed by *auto-rotation*, to display the pattern rotated by $-\omega_s t$.

With the non-translating, non-rotating pattern, any global or local oscillation frequency can be determined as $f_o \approx f_d$ again using temporal sampling.

3 RESULTS

Results of the study of Lenia will be outlined in various sections: Physics, Taxonomy, Ecology, Morphology, Behavior, Physiology, and Case Study.

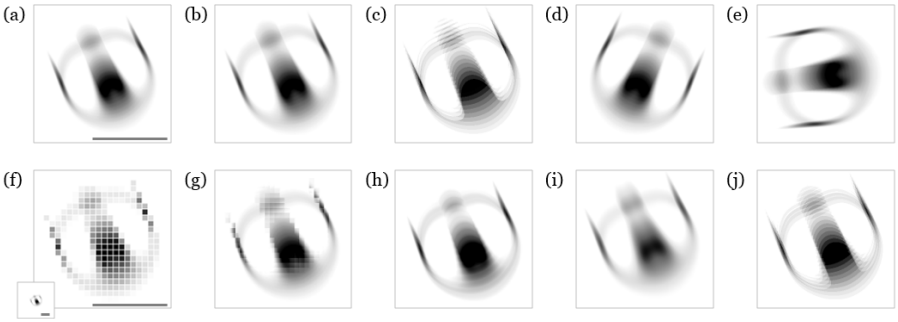

Figure 6: Plasticity of *Orbium* ($\mu = 0.15, \sigma = 0.016$) under various environment settings and transformations. (Scale bar is unit length = kernel radius, same in all panels). **(a)** Original settings: $R = 185, T = 10, P > 10^{15}$ (double precision), exponential core functions. **(b-c)** Core functions changed to polynomial with no visible effect (b), to rectangular produces rougher pattern (c). **(d-e)** Pattern flipped horizontally (d) or rotated 77°anti-clockwise (e) with no visible effect. **(f-g)** Pattern downsampled with space compressed to $R = 15$ (f: zoomed in, inset: actual size), under recovery after upsampled using nearest-neighbor and space resolution restored to $R = 185$ (g), eventually recovers to (a). **(h-i)** Time compressed to $T = 5$ produces rougher pattern (h); time dilated to $T = 320$ produces smoother, lower density pattern (i). **(j)** Fewer states $P = 10$ produces rougher pattern.

3.1 Physics

We present general results regarding the effects of basic CA settings, akin to physics where one studies how the space-time fabric and fundamental laws influence matter and energy.

3.1.1 Spatial invariance

For sufficiently fine space resolution ($R > 12$), patterns in Lenia are minimally affected by spatial similarity transformations including shift, rotation, reflection and scaling (Figure 6(d-g)). Shift invariance exists in all homogenous CAs; reflection invariance is enabled by symmetries in neighborhood and local rule; scaleinvariance is enabled by large neighborhoods (as in LtL [25]); rotation invariance is enabled by circular neighborhoods and totalistic or polar local rules (as in SmoothLife [28] and Lenia). Our empirical data of near constant metrics of *Orbium* over various space resolutions further supports scale invariance in Lenia (Figure 7(a-b)).

3.1.2 Temporal asymptosy

The local rule ϕ of discrete Lenia (DL) can be considered the Euler method $\mathbf{A}_{n+1} = \mathbf{A}_n + hf(\mathbf{A}_n)$ for solving the local rule ϕ of continuous Lenia (CL)

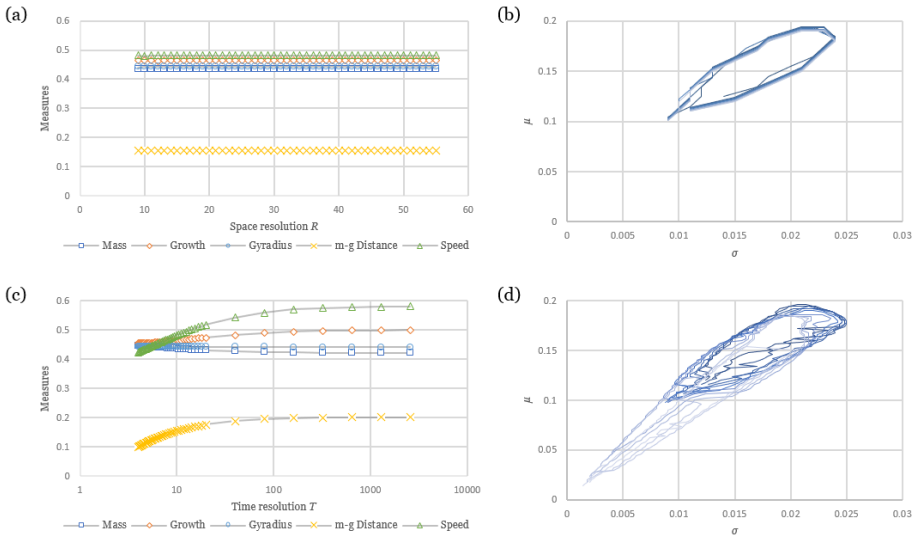

Figure 7: Effects of space-time resolutions as experimented with *Orbium* ($\mu = 0.15, \sigma = 0.016$). Each data point in (a) and (c) is averaged across 300 time-steps. **(a-b)** Spatial invariance: for a range of space resolution $R \in \{9 \dots 55\}$ and fixed time resolution T=10, all statistical measures (mass m, growth g, gyradius r_m, growth-centroid distance d_{gm}, linear speed s_m) remain constant (a) and the parameter range ("niche") remain static (total 557 loci) (b). **(c-d)** Temporal asymptosy: for a range of time resolution $T \in \{4 \dots 2560\}$ and fixed space resolution R=13, structure-related measures (m, r_m) go down and dynamics-related measures (g, d_{gm}, s_m) go up, reaching each continuum limit asymptically (c); the parameter range expands as time dilates (dark to light enclosures, total 14,182 loci) (d).

rewritten as ordinary differential equation (ODE):

$$\mathbf{A}^{t+dt} = \mathbf{A}^t + \mathrm{d}t \left[G(\mathbf{K} * \mathbf{A}^t) \right]_{-\mathbf{A}^t/\mathrm{d}t}^{(1-\mathbf{A}^t)/\mathrm{d}t} \tag{19}$$

$$\frac{\mathrm{d}}{\mathrm{d}t}\mathbf{A}^t = \left[G(\mathbf{K} * \mathbf{A}^t) \right]_{-\mathbf{A}^t/\mathrm{d}t}^{(1-\mathbf{A}^t)/\mathrm{d}t} \tag{20}$$

The Euler method should better approximate the ODE as step size h diminishes, similarly DL should approach its continuum limit CL as Δt decreases. This is supported by empirical data of asymptotic metrics of *Orbium* over increasing time resolutions (Figure 7(c-d)) towards an imaginable "true *Orbium*" (Figure 6(i)).

3.1.3 Core functions

Choices of kernel core K_C and growth mapping G (the core functions or "fundamental laws") alters the "textures" of a pattern but not its overall structure and

dynamics (Figure 6(b-c)). Smoother core functions (e.g. exponential) produce smoother patterns, rougher ones (e.g. rectangular) produce rougher patterns. This plasticity suggests that similar lifeforms should exist in SmoothLife which resembles Lenia with rectangular core functions, as supported by similar creatures found in both CAs (Figure 1(f-g)).

3.2 Taxonomy

We present the classification of Lenia lifeforms into a hierarchical taxonomy, a process comparable to the biological classification of Terrestrial life [38].

3.2.1 Phylogeny of the glider

The most famous moving pattern in GoL is the diagonally-moving "glider" (Figure 1(a)). It was not until LtL [26] that scalable digital creatures were discovered including the glider analogue "bugs with stomach", and SmoothLife [28] was the first to produce an omni-directional bug called the "smooth glider" (Figure 1(f)), which was rediscovered in Lenia as *Scutium* plus variants (Figure 1(e-g) left). We propose the phylogeny of the glider:

> Glider → Bug with stomach → Smooth glider → *Scutium* and variants

Phylogenies of other creatures are possible, like the "wobbly glider" and *Pyroscutium* (Figure 1(f-g) right).

3.2.2 Classification

Principally there are infinitely many types of lifeforms in Lenia, but a range of visually and statistically similar lifeforms were grouped into a *species*, defined such that one *instance* can be morphed smoothly into another by continuously adjusting parameters or other settings. Species were further grouped into higher *taxonomic ranks* — genera, families, orders, classes — with decreasing similarity and increasing generality, finally subsumed into phylum Lenia, kingdom Automata, domain Simulata, and the root Artificialia. Potentially other kinds of artificial life can be incorporated into this Artificialia tree (see Appendix A).

Below are the current definitions of the taxonomic ranks.

- A *species* is a group of lifeforms with the same morphology and behavior in global and local scales, form a cluster (niche) in the parameter space, and follow the same statistical trends in the phase space (Figure 9, 14). Continuous morphing among members is possible.
- A *genus* is a group of species with the same global morphology and behavior but differ locally, occupy adjacent niches, and have discontinuity in statistical trends. Abrupt but reversible transformation among member species is possible.
- A *subfamily* (or *series*) is a series of genera with increasing number of "units" or "vacuoles", occupy parallel niches of similar shapes.

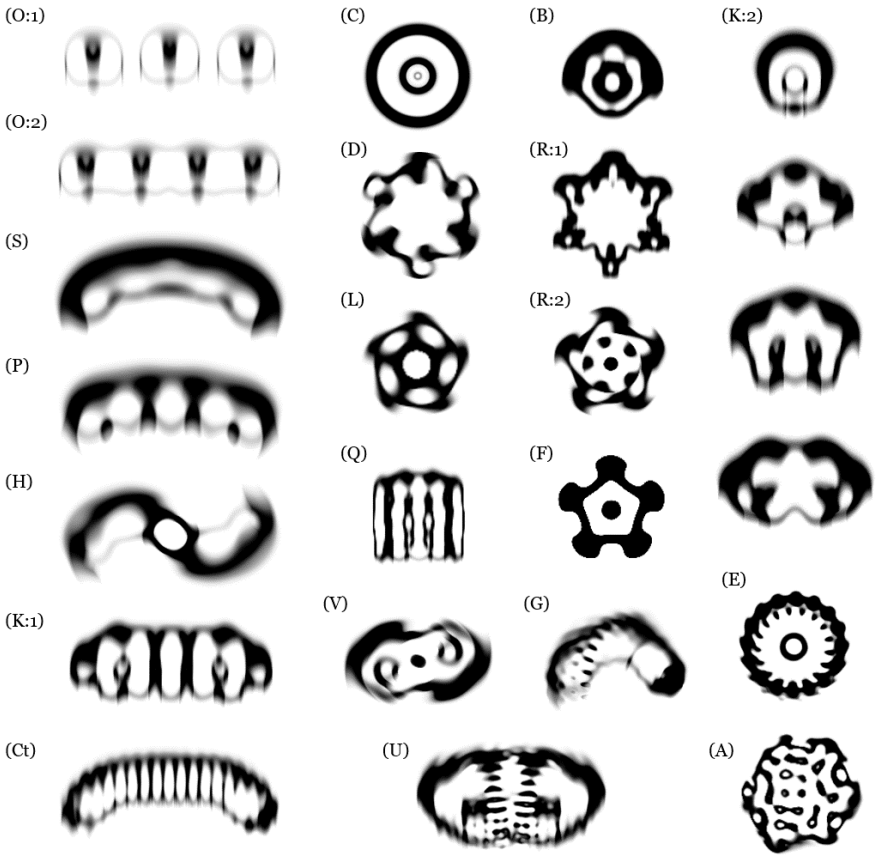

Figure 8: Biodiversity in Lenia as exemplified by the 18 Lenia families (not to scale). **(Column 1)** (O) Orbidae, (S) Scutidae, (P) Pterifera, (H) Helicidae, (K) Kronidae, (Ct) Ctenidae; **(Column 2)** (C) Circidae, (D) Dentidae, (L) Lapillidae, (Q) Quadridae, (V) Volvidae; **(Column 3)** (B) Bullidae, (R) Radiidae, (F) Folidae, (G) Geminidae, (U) Uridae; **(Column 4)** (K) Kronidae, (E) Echinidae, (A) Amoebidae. See Appendix B for details.

- A *family* is a collection of subfamilies with the same architecture or body plan, composed of the same set of components arranged in similar ways.
- An *order* is a rough grouping of families with similar architectures and statistical qualities, e.g. speed.
- A *class* is a high-level grouping of how lifeforms influenced by the arrangement of kernel.

Appendix A gives a proposed taxonomic tree of Lenia according to the above taxonomical ranks, and a proposed "tree of artificial life" in a boarder context. Appendix B gives the details of classes and families.

Much like real-world biology, the taxonomy of Lenia is tentative and is subject to revisions or redefinitions when more data is available.

3.2.3 Naming

Following Theo Jansen for naming artificial life using biological nomenclature (*Animaris* spp.) [39], each Lenia species was given a binomial name that describes its geometric shape (genus name) and behavior (species name) to facilitate analysis and communication. Alphanumeric code was given in the form "*BGUs*" with initials of genus or family name (G) and species name (s), number of units (U), and rank (B).

Suffix "-*ium*" in genus names is reminiscent of a bacterium or chemical elements, while suffixes "-inae" (subfamily), "-idae" (family), and "-iformes" (order) were borrowed from actual animal taxa. Numeric prefix [5] in genus names indicates the number of units, similar to organic compounds and elements (IUPAC names)

3.3 Ecology

We describe the parameter space of Lenia ("geography") and the distribution of lifeforms ("ecology").

3.3.1 Landscapes

The four classes of CA rules [40, 17] corresponds to the four *landscapes* in the Lenia parameter space (Figure 9):

- Class 1 (homogenous "desert") produces no global or local pattern but a homogeneous (empty) state
- Class 2 (cyclic "savannah") produces regional, periodic immobile patterns (e.g. Circidae)
- Class 3 (chaotic "forest") produces chaotic, aperiodic global filament network ("vegetation")
- Class 4 (complex "river") generates localized complex structures (lifeforms)

3.3.2 Niches

In the $(B+1)$-dimensional μ-σ-β parameter hyperspace, a lifeform only exists in a continuous parameter range called its *niche*. Each combination of parameters is called a *locus* (plural: loci).

For a given β, a μ-σ *map* is created by plotting the niches of selected lifeforms on a μ vs. σ chart. Maps of rank-1 species have been extensively charted and were used in taxonomical analysis (Figure 9).

[5] Prefixes used are: *Di-, Tri-, Tetra-, Penta-, Hexa-, Hepta-, Octa-, Nona-, Deca-, Undeca-, Dodeca-, Trideca-*, etc.

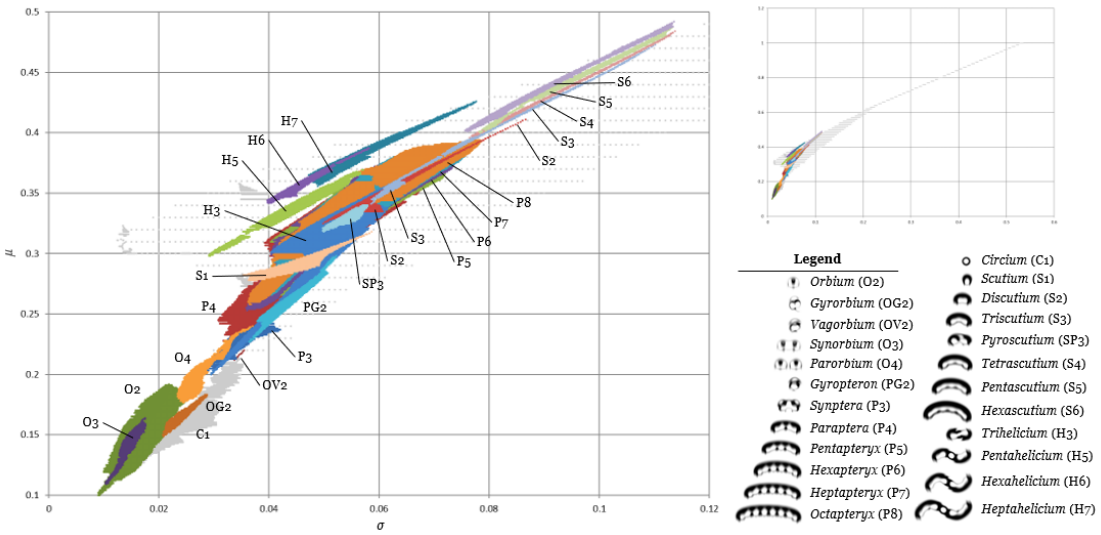

Figure 9: The μ-σ parameter space as μ-σ map, with niches of rank-1 species. Total 142,338 loci. **(legend)** Corresponding names and shapes for the species codes in the map. **(inset)** Wider μ-σ map showing the niche of *Circium* (grey region), demonstrates the four landscapes of rule space: class 1 homogenous desert (upper-left), class 2 cyclic savannah (central grey), class 3 chaotic forest (lower-right), class 4 complex river (central colored).

A *β-cube* is created by marking the existence (or the size of μ-σ niche) of a lifeform at every β locus. As noted in "Definition" section, a B-dimensional hypercube can be reduced to its $(B-1)$-dimensional hypersurfaces, perfect for visualization in the three-dimensional case (Figure 10).

3.4 Morphology

We present the study of structural characteristics, or "morphology", of Lenia lifeforms. See Figure 8 and Appendix B for the family codes (O, S, P, etc.).

3.4.1 Architecture

The structures of Lenia lifeforms can be summarized into the following types of architecture:

- *Segmented architecture* is the serial combination of a few basic components. It is prevalent in class Exokernel (O, S, P, H; also: Ct, U, K). Details in "Anatomy" and "Metamerism" below.
- *Radial architecture* is the radial arrangement of repeating units. It is the defining architecture of Radiiformes in class Endokernel (D, R, B, L, F; also: C, V). Details in "Symmetry" below.

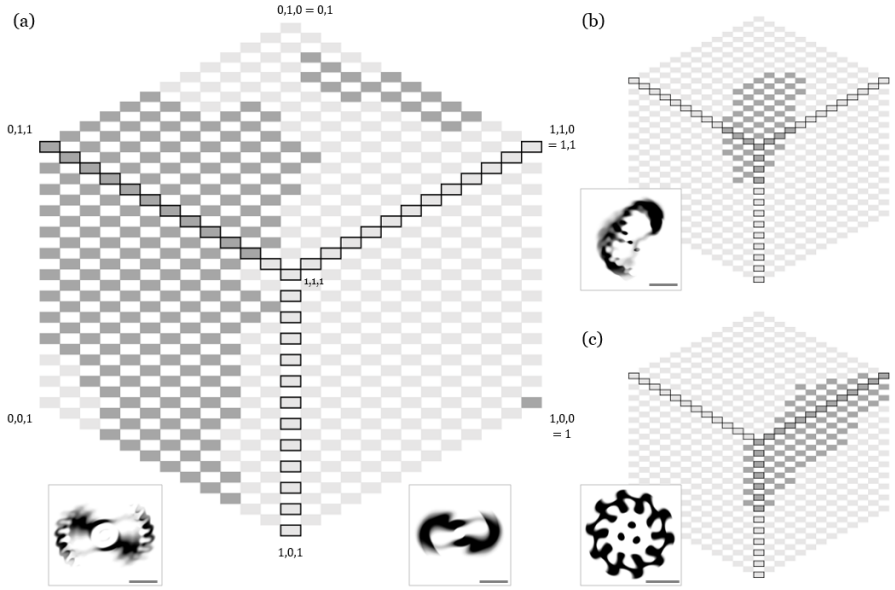

Figure 10: The β parameter space as β-cubes, with niches of selected species from the three Lenia classes. **(a)** β-cube of class Exokernel exemplified by *Helicium*, including rank-1 (right inset) niche at corner $(1, 0, 0)$, rank-2 (left inset) niche at edge near $(1/2, 1, 0)$, rank-3 niche on surfaces near $(1/2, 1/2, 1)$. **(b)** β-cube of class Mesokernel exemplified by *Gyrogeminium gyans* (inset), niche around $(1, 1, 1)$. **(c)** β-cube of class Endokernel exemplified by *Decadentium rotans* (inset), niche mostly on surface $(1, \beta_2, \beta_3)$.

- *Swarm architecture* is the versatile and volatile structure formed by a cluster of granular masses. They are not confined to a particular geometry or locomotive tendency, in extreme case formless and directionless. Common in class Mesokernel (E, G; also: Q, A).

3.4.2 Anatomy

The following is an inventory of components found in segmented species of class Exokernel. Their internal structures or "anatomy" are described (Figure 11(a-c, f)).

- The *orb* (disk) is a circular disk divided into two halves by a central stalk, has a front mouth and a rear tail (plus two side tails). Can be found as singular *Orbium* or compound Orbidae.
- The *scutum* (shield, plural: scuta) is a circular disk with a thick, dense shield at the front, sometimes with an opening (valve). Can be found as singular *Scutium* or compound Scutidae.
- The *wing* or *pteron* (plural: ptera) comes in two flavors:

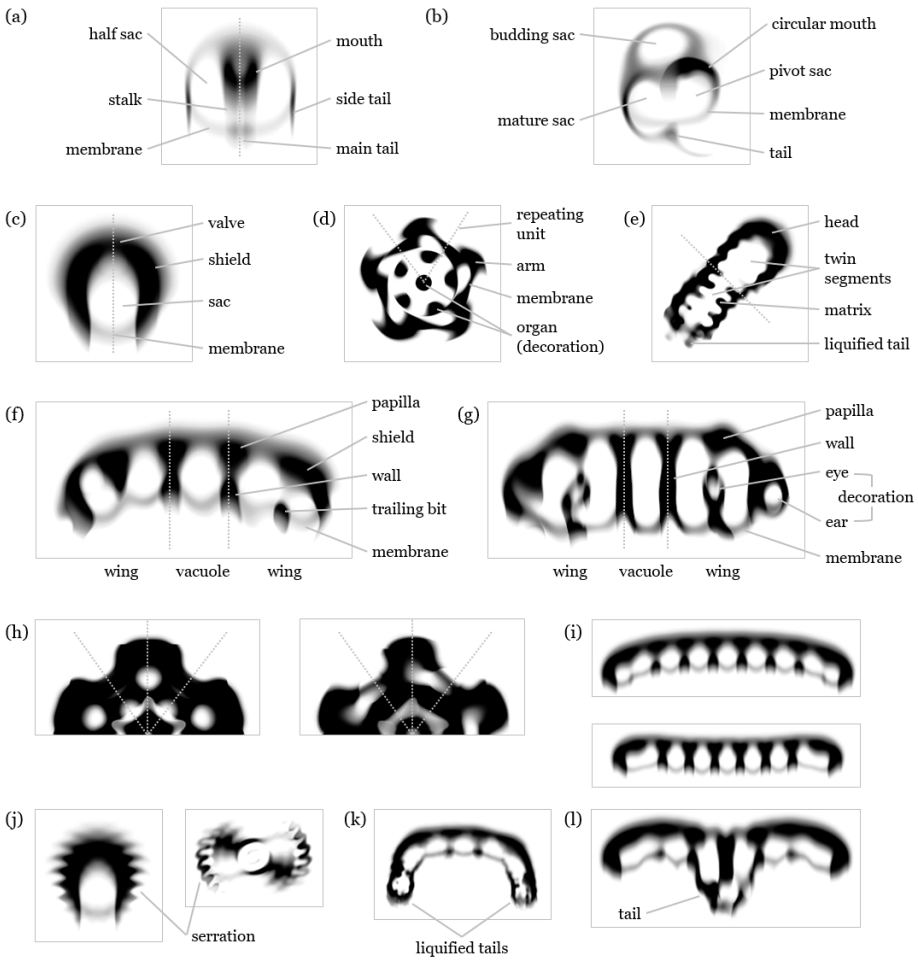

Figure 11: Morphologies and symmetries in Lenia lifeforms (not to scale). **(a-c)** Simple species as standalone components: *Orbium* as standalone orb (a); *Gyrorbium* as standalone orboid wing (b); *Scutium* as standalone scutum (c). **(d-g)** Complex species: radial *Asterium rotans* (d); roughly bilateral *Hydrogeminium natans* (e); long-chain *Pentapteryx* (f) and *Pentakronium* (g). **(h)** Symmetry of radial units: bilateral units in stationary *Asterium inversus* (left) and asymmetric units in rotational *A. torquens* (right). **(i)** Convexity: convex *Nonapteryx arcus* (top) and concave *N. cavus* (bottom). **(j-l)** Ornamentation: serration in higher-rank *Scutium* and *Helicium* (j); liquefaction in *Heptageminium natans* (k), also (e); caudation in *Octacaudopteryx* (l).

– The *orboid wing* (disk-like wing) is a distorted orb with a pivot sac, has a budding mechanism to create a new sac in each cycle, which becomes mature and finally dissolved at the tail. Can be found as

singular *Gyrorbium* or in concave Scutiformes.
  - The *scutoid wing* (shield-like wing) is a distorted scutum with portions of the shield missing. Can be found as singular *Gyropteron* or in convex Scutiformes.
- The *vacuole* (sac) is a circular disk found between two wings in long-chain Scutiformes, with thick walls between vacuoles and wings.

It is likely that many of the components are interrelated, e.g. the orboid wing related to the orb as suggested by smooth transition between *Paraptera cavus* and *Parorbium*; the scutoid wing related to the scutum as suggested by similarity between *Paraptera arcus* and *Tetrascutium*.

3.4.3 Metamerism and convexity

In segmented architecture, multiple components can be combined serially through fusion or adhesion, in a fashion comparable to *metamerism* in biology (or *multicellularity* if we consider the components as "cells") (Figure 11(f-g, i)).

- *Fusion* of multiple orbs (shared halves) forms long-chain Synorbinae; fusion of two orboid wings (shared pivot sac) forms linear *Synptera* or rotating *Helicium*.
- *Adhesion* of multiple orbs forms long-chain Parorbinae; of multiple scuta forms Megaloscutinae; of two wings plus vacuoles forms Vacuopterinae or Helicidae.

Long-chain species exhibit different degrees of *convexity*, especially obvious in longer chains (Figure 11(i)). When ordered by convexity: Scutidae > convex Pteridae (*arcus* subgenus) > linear Orbidae > concave Pteridae (*cavus* subgenus) (Figure 8 column 1). Sinusoidal Pteridae (*sinus* subgenus) have hybrid convexity.

Higher-rank segmented Ctenidae, Uridae, Kronidae also exhibit linear metamerism and convexity with more complicated set of components.

3.4.4 Symmetry and asymmetry

Structural symmetry is a prominent characteristic of Lenia life, including the following types:

- *Bilateral symmetry* (dihedral group D1) is present in segmented architecture (O, S, P, Ct, U, K), also weakly bilateral in some with swarm architecture (G, Q, E).
- *Radial symmetry* (dihedral group Dn) is rotational plus reflectional symmetry, caused by bilateral repeating units in radial architecture (R, L, F), also weakly radial in some with swarm architecture (E).
- *Rotational symmetry* (cyclic group Cn) is rotational without reflectional symmetry, caused by asymmetric repeating units in radial architecture (D, R, L) (Figure 11(h)).

- *Spherical symmetry* (orthogonal group O(2)) is a special case of radial symmetry (C).
- Secondary symmetries:
  - *Spiral symmetry* is secondary rotational symmetry derived from twisted bilaterals (H, V).
  - *Biradial symmetry* is secondary bilateral symmetry derived from radials (B, R).
  - *Deformed bilateral symmetry* is bilateral with heavy asymmetry (e.g. in O, S, Q).
- *Asymmetry* is present in amorphous species (A).

Asymmetry also plays a significant role in shaping the lifeforms and guiding their movements, causing various degrees of angular movements (detailed in "Physiology" section).

Asymmetry is usually intrinsic in a species, as demonstrated by experiments where a slightly asymmetric form (e.g. *Paraptera pedes*, *Echinium limus*) was mirrored into perfect symmetry and remained metastable, but slowly restored to its natural asymmetric form after the slightest perturbation (e.g. rotate by 1°).

3.4.5 Ornamentation

Many detailed local patterns arise in higher-rank species owing to their complex kernels (Figure 11(d-e, j-l)):

- *Decoration* is the addition of tiny ornaments (e.g. dots, circles, crosses), prevalent in class Endokernel.
- *Serration* is a ripple-like sinusoidal boundary or pattern, common in class Exokernel and Mesokernel.
- *Caudation* is a tail-like structure behind a long-chain lifeform (e.g. P, K, U), akin to "tag-along" in GoL.
- *Liquefaction* is the degradation of an otherwise regular structure into a chaotic "liquified" tail.

3.5 Behavior

We present the study of dynamical behaviors of Lenia lifeforms, or "ethology", in analogy to the study of animal behaviors in biology.

3.5.1 Locomotion

Pattern movements in GoL include stationary (fixed, oscillation), directional (orthogonal, diagonal, rarely oblique), and indefinite growth (linear, sawtooth, quadratic) [21]. SmoothLife added omnidirectional movement to the list [28]. Lenia supports a qualitatively different repertoire of behavioral dynamics, which can be described in two levels: global locomotion and local gaits.

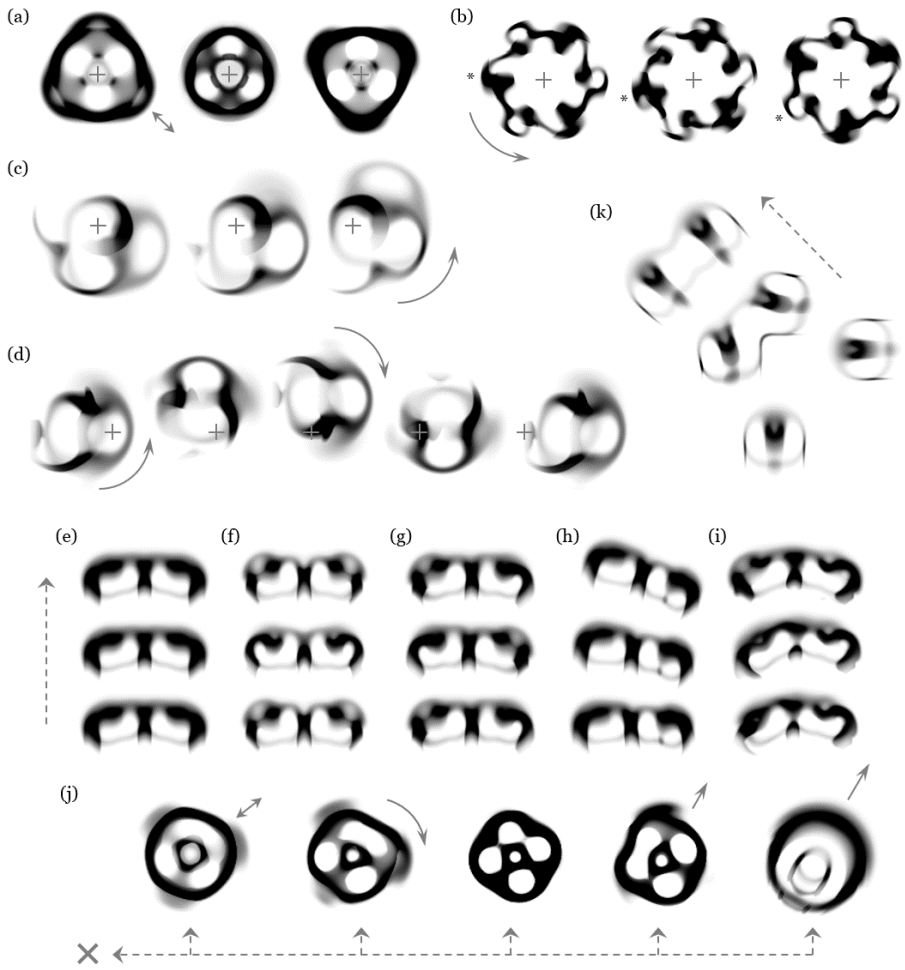

Figure 12: Behavioral dynamics in Lenia lifeforms. (not to scale; + = reference point; → = motion; ⇢ = time flow, left to right if unspecified) **(a)** Stationarity: inverting *Trilapillium inversus* (S_O). **(b)** Rotation: twinkling *Hexadentium scintillans* (R_A) (∗ = same unit). **(c-d)** Gyration: gyrating *Gyrorbium gyrans* (G_O) (c); zigzagging *Vagorbium undulatus* (G_A) (d). **(e-i)** Translocation with gaits: sliding *Paraptera cavus labens* (T_F) (e); jumping *P. c. saliens* (T_O) (f); walking *P. c. pedes* (T_A) (g); deflected *P. sinus pedes* (T_{DA}) (h); chaotic *P. s. pedes rupturus* (T_{CDA}) (i). **(j)** Spontaneous metamorphosis: *Tetralapillium metamorpha* switching among oscillating (S_A), rotating (R_O), frozen (S_F), walking (T_A), and wandering (T_C) (left to right), occasionally die out (×). **(k)** Particle reactions: two *Orbium* collide and fuse together into an intermediate, then stabilize into one *Synorbium*.

The overall movement of lifeforms can be summarized into *modes of locomotion* (Figure 12(a-c, e)):

- *Stationarity* (S) means the pattern stays still with negligible directional movement or rotation.
- *Rotation* (R) is the angular movement around the centroid which has minimal movement.
- *Translocation* (T) is the linear movement in certain direction.
- *Gyration* (G) is the angular movement around a non-centroid center, basically a combination of translocation and rotation.

In formula,

$$\mathbf{A}^{t+\tau} \approx (S_{s\tau} \circ R_{\omega\tau})(\mathbf{A}^t) \tag{21}$$

where τ is the quasi-period, S is a shift by distance $s\tau$ due to linear speed s, R is a rotation (around the centroid) by angle $\omega\tau$ due to angular speed ω.

Stationarity:	$s = 0, \omega = 0$
Rotation:	$s = 0, \omega > 0$
Translocation:	$s > 0, \omega = 0$
Gyration:	$s > 0, \omega > 0$

3.5.2 Gaits

The local details of movements are identified as different *gaits* (Figure 12(e-i)):

- *Fixation* ($_{\mathrm{F}}$) means negligible or no fluctuation during locomotion.
- *Oscillation* ($_{\mathrm{O}}$) is the periodic fluctuation during locomotion
- *Alternation* ($_{\mathrm{A}}$) is the global oscillation plus out-of-phase local oscillations (see "Physiology" section).
- *Deviation* ($_{\mathrm{D}}$) is a small departure from the regular locomotion, e.g. slightly curved linear movement, slight movements in the rotating or gyrating center.
- *Chaoticity* ($_{\mathrm{C}}$) is the chaotic, aperiodic movements during any mode of locomotion.

Any gait or gait combination can be applied to any locomotive mode (e.g. chaotic deviated alternating translocation) and is represented by the combined code (e.g. $\mathrm{T}_{\mathrm{CDA}}$). See Table 2 for possible combinations.

3.5.3 Metamorphosis

Spontaneous metamorphosis is a highly chaotic behavior in Lenia, where a "shapeshifting" species frequently switch among different morphological-behavioral *templates*, forming a continuous-time Markov chain. Each template often resembles an existing species. The set of possible templates and the transition probabilities matrix are determined by the species and parameter values (Figure 12(j)).

Gait (Asymmetry)	Locomotive mode (Symmetry)			
	Stationarity (Radial)	Rotation (Rotational)	Translocation (Bilateral)	Gyration (Deformed bilateral)
Fixation (Static)	S_F = Frozen *Pentafolium lithos*	R_F = Rotating *Asterium rotans*	T_F = Sliding *Paraptera cavus labens* (e)	G_F = Spinning *Gyropteron serratus velox*
Oscillation (Dynamical)	S_O = Ventilating *Hexalapillium ventilans*	R_O = Torqueing *Asterium torquens*	T_O = Jumping *Paraptera cavus saliens* (f)	G_O = Gyrating *Gyrorbium gyrans* (c)
Alternation (Out-of-phase)	S_A = Inverting *Trilapillium inversus* (a)	R_A = Twinkling *Hexadentium scintillans* (b)	T_A = Walking *Paraptera cavus pedes* (g)	G_A = Zigzagging *Vagorbium undulatus* (d)
Deviation (Unbalanced)	S_D = Drifting *Octafolium tardus*	R_D = Precessing *Nivium incarceratus*	T_D = Deflected *Paraptera sinus pedes* (h)	G_D = Revolving *Gyrorbium revolvens*
Chaoticity (Stochastic)	S_C = Vibrating *Asterium nausia*	R_C = Tumbling *Decadentium volubilis*	T_C = Wandering *Paraptera s. p. rupturus* (i)	G_C = Swirling *Gyrogeminium velox*

Table 2: Correlation matrix of symmetries, asymmetries, locomotive modes, and gaits. Each combination is provided with a descriptive term and a sample species. (Parentheses indicate sub-figures in Figure 12.

An extreme form of spontaneous metamorphosis is exhibited by the Amoebidae, where the structure and locomotive patterns are no longer recognizable, while a bounded size can still be maintained.

These stochastic or amoeboid behaviors denied the previous assumption that morphologies and behaviors are fixed qualities in a species, but are actually probabilistic (albeit the probability usually close to one).

3.5.4 Indefinite growth

Besides the limited and controlled behaviors mentioned above where the total mass remains bounded and non-zero, there are unlimited behaviors with indefinite growth or shrinkage.

- *Explosion* is the uncontrolled indefinite growth where the mass quickly expands in all directions, forming a chaotic "vegetation" (cf. class 3 CA).
- *Evaporation* is the uncontrolled indefinite shrinkage where insufficient growth causes the pattern to vanish eventually (cf. class 1 CA).
- *Elongation* is the controllable indefinite growth where a long-chain lifeform keeps lengthening along tangential directions.
- *Contraction* is the controllable indefinite shrinkage where a long-chain lifeform keeps shortening along tangential directions until vanished.

Elongation and contraction are complementary behaviors utilized to evolve long-chain species of desired lengths. Microscopically, vacuoles in the long-chain are being constantly created or absorbed via binary fission or fusion.

Growth rates were estimated by time-series of mass. Linear and circular elongation show linear growth; spiral elongation (in Helicidae) and explosion show quadratic growth. Same for negative growth rates in case of contraction and evaporation.

3.5.5 Particle reactions

Using the interactive program as "particle collider", we investigated the reactions among individual lifeforms especially Orbidae acting as physical or chemical particles. These particles often exhibit elasticity and resilience during collision, engage in inelastic (sticky) collision, and seem to exert a kind of weak "attractive force" when two particles are nearby or a "repulsive force" when getting too close.

Collision of two *Orbium* particles with different incident angles and starting positions would result in one of the followings:

- *Deflection*, two *Orbium* disperse in different angles.
- *Reflection*, one *Orbium* retains its course while one *Orbium* bounces back in opposite direction.
- *Fusion*, two *Orbium* fuse together into one *Synorbium* (Figure 12(k)).
- *Absorption*, two *Orbium* form an unstable intermediate and then only one *Orbium* survives.
- *Annihilation*, the resultant mass evaporates.
- *Detonation*, the resultant mass explodes into infinite growing vegetation.

Starting from a composite Orbidae, the following outcomes are possible:

- *Fission*, one Synorbinae breaks down into multiple smaller Synorbinae or *Orbium*.
- *Parallelism*, multiple *Orbium* travel in parallel with "forces" subtly balanced, forming a Parorbinae.

3.6 Physiology

The exact mechanisms, or "physiology", of morphogenesis (self-organization) and homeostasis (self-regulation) in Lenia are not well understood. Here we will present a few observations and speculations.

3.6.1 Symmetries and behaviors

A striking result in analyzing Lenia is the correlations between structural symmetries/asymmetries ("Morphology" section) and behavioral dynamics ("Behavior" section).

At a global scale, the locomotive modes correspond to the types of overall symmetry.

- Stationarity is associated with radial symmetry (including spherical symmetry).
- Rotation is associated with rotational symmetry (including secondary spiral symmetry).
- Translocation is associated with bilateral symmetry (including secondary biradial symmetry).
- Gyration is associated with deformed bilateral symmetry.

At a local scale, the locomotive gaits correspond to the dynamical developments of asymmetry.

- Fixation implies that any asymmetry remains static.
- Oscillation implies that the asymmetry changes over time.
- Alternation implies that the asymmetries between units are dynamically out of phase.
- Deviation implies that the net balance of asymmetries is unevenly distributed among units.
- Chaoticity implies a stochastic component in the development of asymmetry.

These correlations (Table 2) hold in most conditions, except e.g. a bilateral species that is stationary.

3.6.2 Stability-motility hypothesis

A closer look in the symmetry-behavior correlations suggests the mechanisms of how motions arise.

- A bilateral species has reflectional symmetry along the lateral (left-right) axis, but heavy asymmetry along the longitudinal (rostro-caudal) axis that may be the cause of directional movement along this axis.
- A deformed bilateral species has the lateral reflectional symmetry broken, that introduce an angular component to its linear motion.
- A radial species has bilateral repeating units arranged radially, all directional vectors along the radii (either pulling in to or pushing out from the centroid) cancel out, thus overall remain stationary.
- A rotational species has asymmetric repeating units with lateral reflectional symmetry broken, that initiates an angular rotation around the centroid.

On top of these global movements, the dynamical qualities of asymmetry — static/dynamical, in-phase/out-of-phase, balanced/unbalanced, regular/stochastic — lead to the dynamical qualities of locomotion (i.e. gaits).

Based on these reasonings, we propose the following *stability-motility hypothesis* in Lenia (potentially applicable to real-world physiology or evolutionary biology):

> Symmetry provides stability; asymmetry provides motility.
>
> Distribution of asymmetry determines locomotive mode; its development determines gait.

3.6.3 Alternation and internal communication

The alternation gait, that is global oscillation plus out-of-phase local oscillations, demonstrates phenomena like long-range synchronization and internal

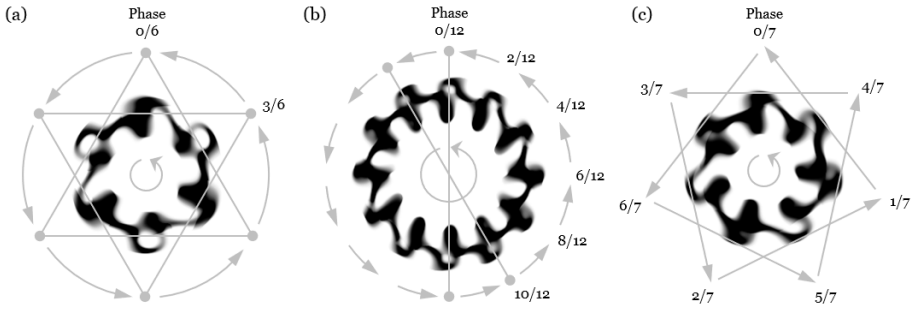

Figure 13: "Internal clockwork" in selected alternating Dentidae species. After $1/n$ cycle, all phases advance by $1/n$ while phase relations remain unchanged. (not to scale; $\rightarrow$ = phase transfer; $\multimap$ = same phase; $\circlearrowleft$ = rotation, taken as the positive direction) **(a)** Even-sided *Hexadentium scintillans*, with opposite-phase adjacent units and in-phase alternating units. **(b)** Even-sided *Dodecadentium scintillans*, with sequentially out-of-phase adjacent units and in-phase opposite units. **(c)** Odd-sided *Heptadentium scintillans*, with globalized phase distribution.

clockwork, suggests the existence of self-organization and internal communication among components.

Alternating translocation ($\mathrm{T_A}$) in a simple bilateral species, where the two halves are in opposite phases, leads to spatiotemporal reflectional (i.e. glide) symmetry at half-cycle, in addition to the full oscillation

$$\mathbf{A}^{t+\tau/2} \approx (S_{s\tau/2} \circ F)(\mathbf{A}^t) \tag{22}$$

$$\mathbf{A}^{t+\tau} \approx S_{s\tau}(\mathbf{A}^t) \tag{23}$$

where τ is the quasi-period, S is a shift, F is a flip (along the lateral axis). (Figure 12(g))

Genus (species *scintillans*)	Rank (B)	Units (n)	Phase difference (k/n cycle) between adjacent units	Rotational symmetry (angle $m \cdot 2\pi/n = m$ units) between $1/n$ cycle
Hexadentium (a)	2	6	3/6	$1 \cdot 2\pi/6$ = adjacent
Heptadentium (c)	2	7	4/7	$2 \cdot 2\pi/7$ = skipping
Octadentium	2	8	4/8	$1 \cdot 2\pi/8$ = adjacent
Nonadentium	2	9	5/9	$2 \cdot 2\pi/9$ = skipping
Decadentium	4	10	2/10	$1 \cdot 2\pi/10$ = adjacent
Undecadentium	4	11	2/11	$6 \cdot 2\pi/11$ = skipping
Dodecadentium (b)	4	12	2/12	$1 \cdot 2\pi/12$ = adjacent
Tridecadentium	4	13	3/13	$9 \cdot 2\pi/13$ = skipping

Table 3: Alternation characteristics (B, n, k, m) in selected alternating Dentidae species. (Parentheses indicate sub-figures in Figure 13)

In alternating long-chain species, where the two wings are oscillating out-of-phase but the main chain remains static, demonstrates *long-range synchronization* that faraway local structures are able to synchronize with each other. [6]

Alternating gyration ($\mathrm{G_A}$) is a special case only found in *Vagorbium* (a variant of *Gyrorbium*) where it gyrates to the opposite direction every second cycle, resulting in a zig-zag trajectory (Figure 12(d)).

Alternating stationarity ($\mathrm{S_A}$) occurs in stationary radial lifeforms (with n repeating units), leads to spatiotemporal reflectional or rotational symmetry at half-cycle, giving an optical illusion of "inverting" motions (Figure 12(a)).

$$\mathbf{A}^{t+\tau/2} \approx F(\mathbf{A}^t) \approx R_{\pi/n}(\mathbf{A}^t) \tag{24}$$

$$\mathbf{A}^{t+\tau} \approx \mathbf{A}^t \tag{25}$$

where R is a rotation (around the centroid).

Alternating rotation ($\mathrm{R_A}$) is an intricate phenomenon found in rotational species, especially family Dentidae. Consider a Dentidae species with n repeating units, two adjacent units are separated spatially by angle $2\pi/n$ and temporally by a phase difference of k/n cycle (Figure 13).

After $1/n$ cycle, the pattern recreates itself with rotation $\omega\tau/n$ due to angular speed ω, plus an extra rotational symmetry of m units (angle $2\pi m/n$) due to alternation, which leads to spatiotemporal rotational symmetry at $1/n$ cycle

$$\mathbf{A}^{t+\tau/n} \approx R_{\omega\tau/n+2\pi m/n}(\mathbf{A}^t) \tag{26}$$

$$\mathbf{A}^{t+\tau} \approx R_{\omega\tau}(\mathbf{A}^t) \tag{27}$$

This giving an optical illusion that local features (e.g. a hole) are being transferred from one unit to another inside the rotating species (Figure 13 outer arrows).

The values of k and m depend on the species, seem to follow no obvious trend, except that $m = 1$ (adjacent phase transfer) in even-sided species and $m > 1$ (unit-skipping) in odd-sided species (Table 3).

3.6.4 Allometry

Besides direct observation, patterns in Lenia can be studied though statistical measurement and analysis, akin to "allometry" or "biostatistics" in biology.

For example, various behaviors can be inferred by the average (mean or median), variability (standard deviation or interquartile length) or phase space trajectory of various statistical measures (Table 4).

A few general trends can be deduced from measure charts, for example, linear speed is found to be roughly inverse proportional to density. From the linear speed vs. mass chart (Figure 14), genera form strata according to linear speed (O>P>S>H>C), and species form clusters according to mass, while cluster

[6] We performed experiments to show that alternation is self-recovering, meaning that it is actively maintained by the species and is not coincidental.

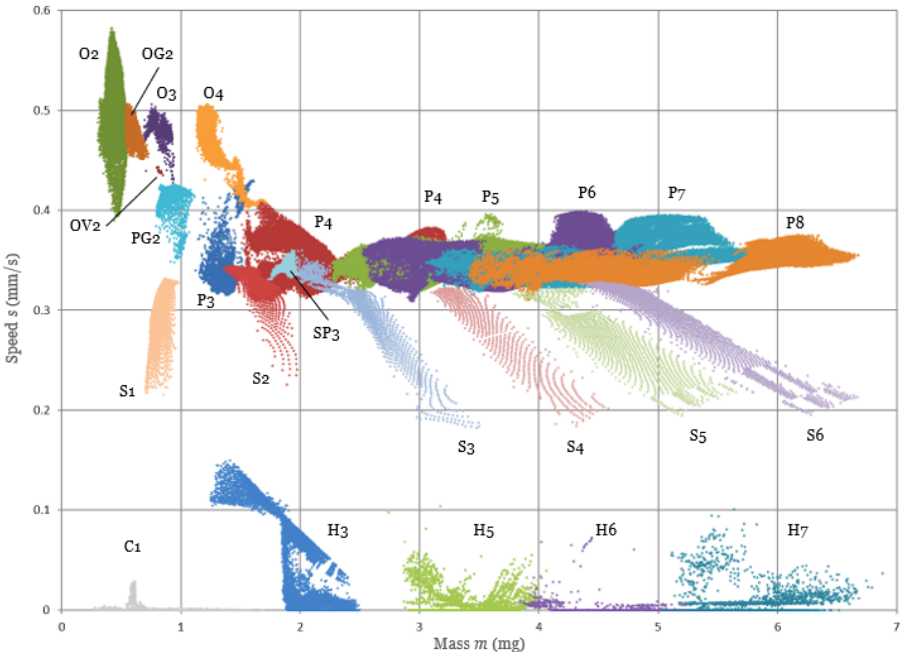

Figure 14: Measure chart of linear speed vs. mass for rank-1 species. Total 142,338 loci, 300 time-steps ($t = 30$s) per locus. See Figure 9 legend for species codes.

shapes may convey further information, e.g. twin clusters indicate a separation in convexity.

3.7 Case Study

In the previous sections, we outlined the general characterizations of Lenia life from various perspectives. Here we combine these aspects and provide a focused study on one representative genus — *Paraptera* — as a concrete example of qualitative and quantitative analysis.

3.7.1 The Unit-4 family

From a wider perspective, *Paraptera* is closely related to two other genera *Parorbium* and *Tetrascutium*, altogether they comprise the rank-1 unit-4 group.

In the μ-σ map (Figure 15), their niches comprise the *Parorbium*-*Paraptera*-*Tetrascutium* complex. The narrow bridge between *Parorbium* and *Paraptera* indicates that continuous transformation is possible, while the correspondence between the small tip on *Paraptera* (species *P. arcus valvatus*) and *Tetrascutium* suggests a remote relationship (as hinted by their similar morphology).

	Measure of linear motion	Measure of angular motion	Measure of oscillation
	s_m	$\lvert m_\Delta \rvert, \omega_m, \omega_s, \ldots$	$m, g, s_m, \ldots$
Locomotion modes			
Stationarity	Average ≈ 0	Average ≈ 0	
Rotation	Average ≈ 0	Average > 0 *	
Translocation	Average > 0	Average ≈ 0	
Gyration	Average > 0	Average > 0	
Gaits			
Fixation			Variability ≈ 0
Oscillation			Variability > 0
Alternation (in translocation)		Variability > 0	
Deviation (in translocation)		Average > 0	
Chaoticity		$\longleftarrow$ Chaotic trajectory $\longrightarrow$	

Table 4: Allometric relationships between behavior and statistical measures. (* = only works in some cases).

Species			Morphology	Behavior
O4	genus *Parorbium* (family Orbidae)			
	O4d	*Po. dividuus*	Two parallel orbs, separated	T = translocating
	O4a	*Po. adhaerens*	Two parallel orbs, adhered	T
P4	genus *Paraptera* (family Pterifera)			
	P4o*	*P. orbis* *	Concave, twin orboid wings	T
	P4c*	*P. cavus* *	Concave, twin orboid wings	T
	P4a*	*P. arcus* *	Convex, twin scutoid wings	T
	P4s*	*P. sinus* *	Sinusoidal, orboid + scutoid wings	T_{D^*} = deflected
	P4*l	*P. * labens*	Bilateral	T_F = sliding
	P4*s	*P. * saliens*	Bilateral	T_O = jumping
	P4*p	*P. * pedes*	Bilateral with slight asymmetry	T_A = walking
	P4*v	*P. * valvatus*	Scutidae-like, twin wings, valving	T_O = valving
	P4**f	*P. * * furiosus*	Occasional stretched wing	T_{C^*} = chaotic
S4	genus *Tetrascutium* (family Scutidae)			
	S4s	*T. solidus*	Four fused scuta, solid	T_F = sliding
	S4v	*T. valvatus*	Four fused scuta, valving	T_O = valving

Table 5: Non-exhausive list of species isolated from the *Parorbium-Paraptera-Tetrascutium* complex. (* = combinations are possible, e.g. P4spf with behavior T_{CDA})

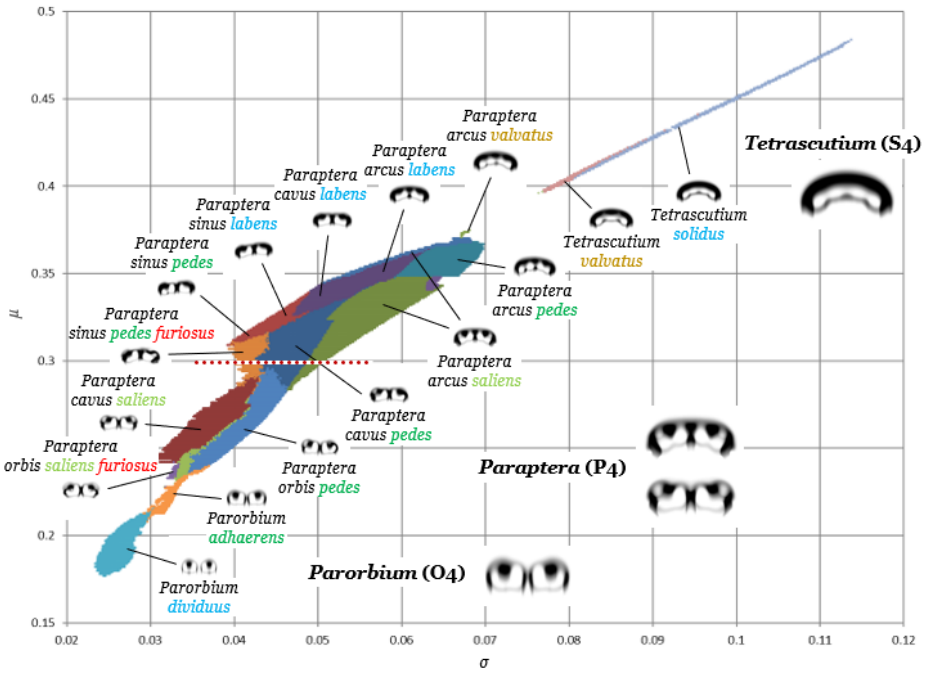

Figure 15: μ-σ map of the unit-4 family, showing the prominent *Parorbium-Paraptera-Tetrascutium* complex. Total 16,011 loci. The red dotted line marks the cross-sectional study (Figure 16).

Allometric methods were employed to further segregate the complex (Figure 16, Table 4). A few potential species with distinct traits (e.g. jumping or walking) were isolated in measure charts. After verified in computer simulations that they exhibit unique morphology or behavior, new species names were assigned (Table 5).

3.7.2 Cross-sectional study

In genus *Paraptera*, a cross section at $\mu = 0.3$ was further studied, where five species exist in $\sigma \in [0.0393, 0.0515]$ (Figure 15 red dotted line, Table 6).

To assess their behavioral traits, five number summaries of statistical mea-

Species		σ range	Morphology and behavior
P4as	*P. arcus saliens*	$[0.0468, 0.0515]$	Convex, jumping (T_O)
P4cp	*P. cavus pedes*	$[0.0412, 0.0483]$	Concave, walking (T_A)
P4sp	*P. sinus pedes*	$[0.0404, 0.0414]$	Sinusoidal, deflected walking (T_{DA})
P4spf	*P. sinus pedes furiosus*	$[0.0400, 0.0403]$	Sinusoidal, chaotic deflected walking (T_{CDA})
P4spr	*P. sinus pedes rupturus*	$[0.0393, 0.0399]$	Sinusoidal, chaotic deflected walking, fragile

Table 6: List of *Paraptera* species in the cross-section studied $\mu = 0.3$.

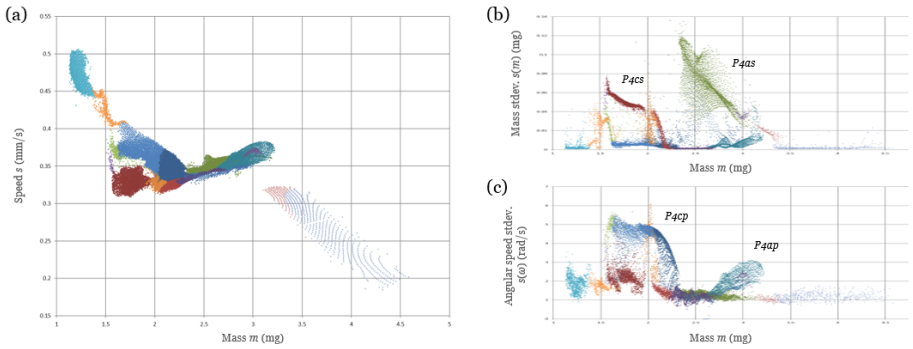

Figure 16: Measure charts of various measures for the unit-4 family. Total 16,011 loci, 300 time-steps ($t = 30$s) per locus. **(a)** Linear speed vs. mass, showing a distribution comparable to the μ-σ map flipped vertically. **(b)** Mass variability vs. mass, isolating the jumping (T_O) species e.g. *Paraptera cavus saliens* (P4cs) and *P. arcus saliens* (P4as). **(c)** Angular speed variability vs. mass, isolating the walking (T_A) species e.g. *P. cavus pedes* (P4cp) and *P. arcus pedes* (P4ap).

sures (mass m and mass asymmetry m_Δ) were plotted against σ, together with snapshot phase space trajectories at a few loci (Figure 17, also see Figure 12(e-i)).

At higher σ values, *Paraptera arcus saliens* (P4as) has high m variability and near zero m_Δ, corresponding to perfect bilateral symmetry and jumping behavior (locus a). *P. cavus pedes* (P4cp) has high m_Δ variability, corresponding to alternating asymmetry and walking behavior (locus d).

P4as and P4cp coexist over $\sigma \in [0.0468, 0.0483]$. Just outside of this niche overlap, the two species slowly transform into each other, as shown by the spiral phase space trajectories (loci b, c). Slow transformations also occur between P4cp and P4sp (locus f).

Irregularity and chaos arise at lower σ values. *P. sinus pedes* (P4sp) has non-zero m_Δ, corresponding to asymmetric morphology and deflected movement (locus g). *P. sinus pedes furiosus* (P4spf) has chaotic phase space trajectory, corresponding to deformed morphology and chaotic movement (locus h).

At the edge of chaoticity, *P. sinus pedes rupturus* (P4spr) has even higher and rugged variability, often encounters episodes of acute deformation but eventually recovers (locus i). Outside the σ lower boundary, the pattern fails to recover and finally disintegrates.

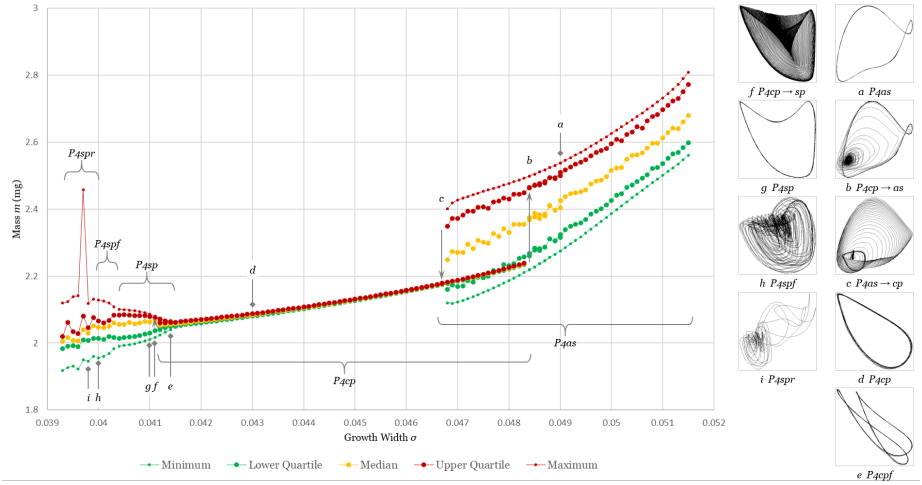

(a)

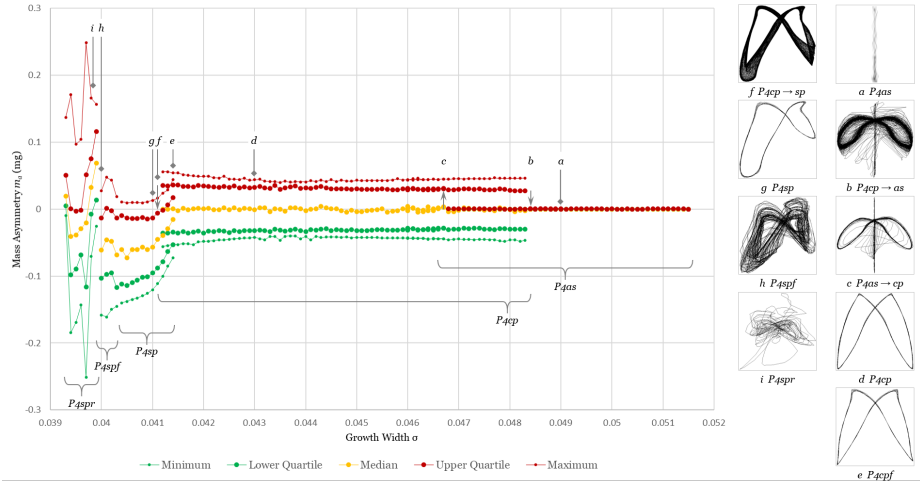

(b)

Figure 17: Cross-sectional charts at $\mu = 0.3, \sigma \in [0.0393, 0.0515]$ in genus *Parapteria*. 200 time-steps ($t = 20$s) per locus (See Table 6 for species codes). **(a)** Mass m vs. parameter σ chart, with phase space trajectories of growth vs. mass (insets) sampled at loci a-i. **(b)** Mass asymmetry m_Δ vs. parameter σ chart, with phase space trajectories of linear speed vs. angular speed (insets) sampled at loci a-i.

Standard CA patterns (e.g. GoL, ECA)		Geometric CA patterns (e.g. LtL, SmoothLife, Lenia)
	Structure	
"Digital"		"Analog"
Localized motifs		Geometric manifolds
Quantized		Smooth
Complex circuitry		Complex combinatorics
	Dynamics	
Deterministic		Unpredictable
Precise		Fuzzy
Strictly periodic		Quasi-periodic
Machine-like		Life-like
	Sensitivity	
Fragile		Resilient
Mutation sensitive		Mutation tolerant
Rule-specific		Rule-generic
Rule change sensitive		Rule change adaptive

Table 7: Contrasting qualities of patterns in standard and geometric CAs.

4 DISCUSSION

4.1 Geometric Cellular Automata

Standard CAs like GoL and ECA consider only the nearest sites as neighborhood, while more recent variants like LtL, SmoothLife and Lenia have extended neighborhoods, and are able to control over the "granularity" of space. The latter ones are still technically discrete, but are likely approximating a continuous class of models called Euclidean automata (EA) [27]. We call them *geometric cellular automata* (GCA).

GCAs and standard CAs are fundamentally different, with a number of contrasting qualities between their generated patterns (Table 7). In standard CAs, a large number of interesting patterns are concentrated in specific rules like GoL, while GCAs patterns are scattered over the parameter space. Also, the distinction of "digital" vs. "analog" goes beyond a metaphor, in that standard CAs like GoL and ECA rule 110 are actually capable of (digital) universal computation [22, 41], while whether a certain kind of "analog computer" is possible in GCAs remains to be seen.

As GCAs being approximants of EAs, these contrasting qualities may well exist between EAs and CAs.

4.2 Nature of Lenia

Here we deep dive into the very nature of Lenia regarding the unpredictability, fuzziness, quasi-periodicity, resilience and lifelikeness of its generated patterns, at times using GoL for contrast.

4.2.1 Persistence and unpredictability

GoL patterns are either persistent, which are guaranteed to follow the same dynamics every time, or temporary, which will eventually stabilize as persistent patterns or vanish. Lenia patterns, on the other hand, have various types of *persistence*:

1. Transient patterns that only last for a short time.
2. Quasi-stable patterns that are able to sustain for a few to hundreds of cycles.
3. Stable patterns that survive as long as simulations went, seemingly everlasting.
4. Metastable patterns that are stable, but transform into other patterns after slight perturbations.
5. Chaotic patterns that "walk a thin line" between chaos and self-destruction.
6. Markovian patterns that shapeshift among templates, each has its own degree of persistence.

Given a static pattern, it is *unpredictable* whether it belongs to which persistent level unless we put it into simulation for a considerable (potentially infinite) amount of time, a situation akin to the halting problem and the undecidability in class 4 CAs [42]. This uncertainty results in the vague niche boundaries of many Lenia species (especially at lower σ values with much chaos).

Even at persistent level 3, in contrast to the "glider" in GoL that will move diagonally forever, we can never be 100% sure that a seemingly stable *Orbium* will not eventually die out.

4.2.2 Fuzziness and essence

No two patterns in Lenia are the same. There are various levels of *fuzziness* and subtle varieties. Within a species, slightly differences in parameters, rule settings, or initial configurations would result in slightly different patterns (see Figure 6). Even during a pattern's lifetime, no two cycles are the same.

Consider the phase space trajectories of recurrent patterns (Figure 18), evidently every trajectory corresponds to an attractor (or a strange attractor if chaotic). Yet, behind a group of similar patterns, there seems to be another kind of "attractor" that draws them into a common morphological-behavioral template.

In philosophy, *essentialism* proposes that every entity in the world can be identified by a set of intrinsic features or an "essence", be it an ideal form (Plato's idealism) or a natural kind (Aristotle's hylomorphism). So in Lenia, is there something like "Orbium-ness" in all instances and occurrences of *Orbium*? Could this be identified or utilized objectively and quantitatively?

The notions of an "attractor" or "essence" and the tolerance of fuzziness around such central tendency is what makes the definition of a Lenia "species" possible.

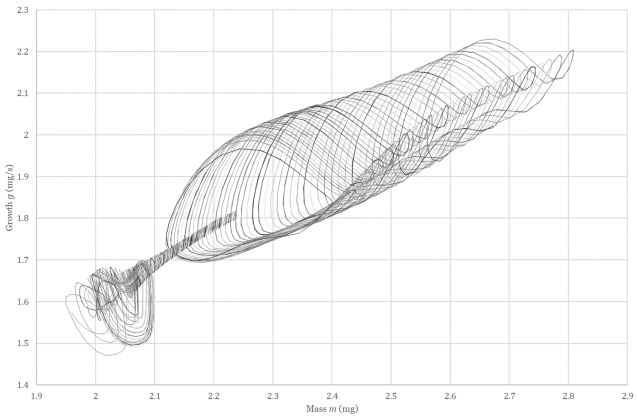

Figure 18: Phase space trajectories of growth vs. mass (same cross-section as Figure 17); trajectories separated by $\Delta\sigma = 0.0001$, each over a period of $t = 20$s. Every trajectory corresponds to an attractor, a group of similar trajectories hints a species-level "attractor".

4.2.3 Quasi-periodicity and recurrence

Unlike GoL where a recurrent pattern returns to the exact same pattern after an exact period of time, a recurrent pattern in Lenia returns to similar patterns after slightly irregular periods or *quasi-periods*, which are probably normally distributed around an average. Lenia has various types of periodicity:

1. Aperiodicity, transient non-recurrent patterns.
2. Quasi-periodicity, quasi-stable, stable or metastable patterns.
3. Chaotic periodicity, chaotic patterns, with wide-spread period distribution.
4. Markovian periodicity, Markovian patterns, each template has its own quasi-period.

Essentially, in discrete Lenia, there are finite, albeit astronomically large, number of possible configurations $|\mathcal{S}^{\mathcal{L}}|$. Given enough time, an initial pattern would eventually return to the exact same pattern, an argument not unlike Nietzsche's "eternal recurrence". But in Lenia, there would be numerous approximate recurrences between two exact recurrences, while in continuous Lenia, exact recurrence may even be impossible.

4.2.4 Plasticity and kernel resonance

Given the fuzziness and irregularity in Lenia patterns, they are surprisingly resilient and exhibit *phenotypic plasticity*. By adjusting their structures and dynamics elastically, they are able to absorb deformations and transformations, adapt to environmental changes (parameters and rule settings), or react to head-to-head collisions, and continue to survive.

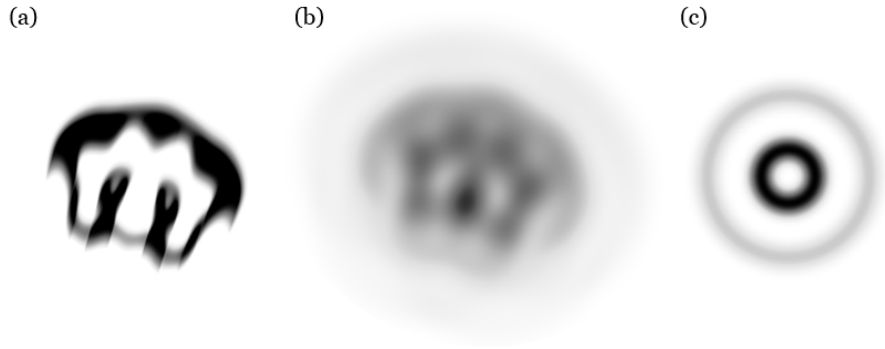

Figure 19: Different views of calculation intermediates. Configuration $\mathbf{A}^t$ (a), potential distribution $\mathbf{U}^t$ (b), and kernel $\mathbf{K}$ (c). Notice one larger and six smaller potential peaks (b: dark spots) possibly formed by kernel resonance, and the corresponding inner spaces (a: white areas).

A speculative mechanism for the plasticity (also self-organization and self-regulation in general) is postulated as the *kernel resonance hypothesis* (Figure 19). In the potential distribution, a network of *potential peaks* can be observed. Possibly, each peak was formed by the overlapping or "resonance" of kernel rings casted by mass lumps from various locations, while the collection of peaks in turn determine the location of the mass lumps. In this way, the mass lumps (i.e. peaks in the mass distribution) influence each other reciprocally and may self-organize into local structures, providing the basis of morphogenesis.

The kernel resonance would be dynamic over time, and may even be self-regulating due to the mass-potential-mass feedback loop, providing the basis of homeostasis. Plasticity may stem from static buffering and dynamical flexibility provided by such feedback loop.

4.3 Connections with Biological Life

Besides the superficial resemblance, Lenia life may have deeper connections with biological life.

4.3.1 Symmetry and locomotion

Both Lenia and Earth life exhibit structural symmetry and similar symmetry-locomotion relationships (Figure 20(b-c)).

Radial symmetry is universal in Lenia order Radiiformes. In biological life, radial symmetry is exhibited in microscopic protists (diatoms, radiolarians) and primitive animals historically grouped as Radiata (jellyfish, corals, comb jellies, echinoderm adults). These radiates are sessile, floating or slow-moving, similarly, Lenia radiates are usually stationary or rotating with little linear movement.

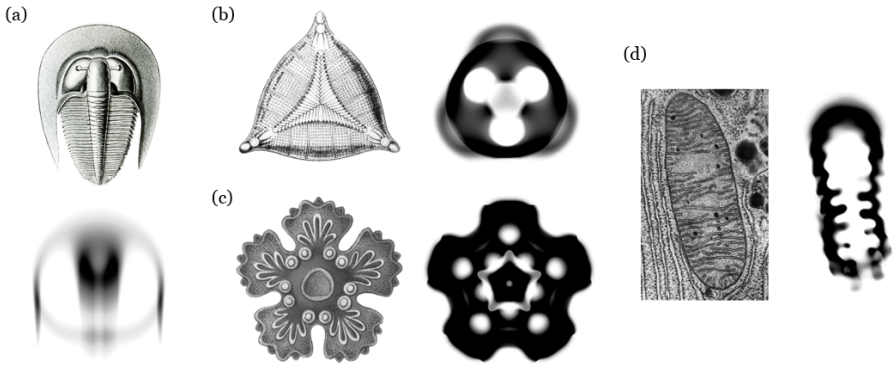

Figure 20: Appearance similarities between Earth and Lenia life. **(a)** Bilateral trilobite *Bohemoharpes ungula* [44, plate 47] and Lenian *Orbium bicaudatus*. **(b)** Trimerous diatom *Triceratium moronense* [44, plate 4] and Lenian *Trilapillium inversus*. **(c)** Pentamerous larva of sea star *Asterias* species [44, plate 40] and Lenian *Asterium inversus*. **(d)** Weakly bilateral mitochondrion [45] and Lenian *Hydrogeminium natans*, with matrix-like internal structures.

Bilateral symmetry is ubiquitous among Lenia families. In biological life, the group Bilateria (vertebrates, arthropods, mollusks, various "worm" phyla) with the same symmetry are the most successful branch of animals since their proliferation and rapid diversification near the Cambrian explosion 542 million years ago [43]. These bilaterians are optimized for efficient directed locomotion, while similarly, Lenia bilaterians engage in fast linear movements.

4.3.2 Adaptation to environment

The parameter space of Lenia, earlier visualized as a geographical landscape ("Ecology" section), can also be thought of as an *adaptive landscape*. Species niches correspond to fitness peaks in the adaptive landscape, indicate successful adaptation of those structural-dynamical templates to ranges of parametric environmental settings.

Among all body plans (correspond to Earth animal phyla or Lenia families), some may be considered more adaptive as indicated by higher biodiversity, wider ecological distribution, and perhaps greater complexity. In Earth life, the champions are the insects (in terms of biodiversity), the nematodes (in terms of ecosystem breadth and individual count), and the mammals (producing intelligent species like cetaceans and primates). In Lenia, family Pterifera is the most successful in class Exokernel with its high diversity (number of species), wide distribution (total niche area), and high complexity.

The parallels between two systems regarding adaptive landscapes and quantitative assessment of adaptability may provide insights in evolutionary biology and evolutionary computation.

4.3.3 Species problem

One common difficulty encountered in the studies of both Earth and Lenia life is the precise definition of a "species", or the *species problem*. In evolutionary biology, several species concepts have been proposed [46]:

- Morphological species, based on phenotypic differentiation [47]
- Phenetic species, based on numerical clustering (cf. phenetics) [48]
- Genetic species, based on genotypic clustering [49]
- Biological species, based on reproductive isolation [50]
- Evolutionary species, based on phylogenetic lineage divergence [51, 52]
- Ecological species, based on niche isolation [53]

Similar concepts are used in combination for species identification in Lenia, including morphological (similar morphology and behavior), phenetic (statistical cluster) and ecological (niche cluster). However, species concepts face problems in various situations, for example, in Lenia's case, species aggregates or convergent evolution, and in Earth's case, niche complex or shapeshifting lifeforms. It remains an open question whether clustering into species and grouping into higher taxa can be carried out objectively and systematically.

4.4 Future Works

4.4.1 Open questions

Here are a few open questions we hope to answer:

1. What are the enabling factors and mechanisms of how self-organization, self-regulation, self-direction, adaptability, etc. emerge in Lenia?
2. How do interesting phenomena like symmetry, metamerism, spontaneous metamorphosis, particle collision, alternation, etc. arise in Lenia?
3. How is Lenia life related to biological life and other forms of artificial life?
4. Can Lenia life be grouped into species and higher taxa objectively and systematically?
5. Does continuous Lenia exist as the continuum limit of discrete Lenia? If so, do corresponding "ideal" lifeforms exist in this Euclidean Automaton?
6. Is Lenia Tuning-complete and capable of universal computation?
7. Is Lenia capable of open-ended evolution that generates unlimited novelty and complexity?
8. Do self-replicating or pattern-emitting lifeforms exist in Lenia?
9. Do lifeforms exist in other variants of Lenia (e.g. 3D)?

To answer these questions, the following approaches of future works are suggested.

4.4.2 More species

For the sheer joy of discovering new species, and for further understanding Lenia and artificial life, we need better capabilities of species discovery and identification.

Automatic and accurate species identification could be achieved via computer vision and pattern recognition using machine learning or deep learning techniques, e.g. by feeding the grid to a convolutional neural networks (CNNs) or feeding the measures time-series to a recurrent neural networks (RNNs).

Interactive evolutionary computation (IEC) currently used for new species discovery could be advanced to allow crowdsourcing, web or mobile applications with intuitive interface would allow online users to simulate, mutate, select and share interesting patterns (cf. Picbreeder [54], Ganbreeder [55]). Web performance and functionality could be improved using WebAssembly, OpenGL, TensorFlow.js, etc.

Alternatively, *evolutionary computation* (EC) and similar methodologies could be used for automatic and efficient exploration of the search space, as has been successfully used for evolving new body parts or body plans [39, 9, 56]. Patterns could be represented in genetic (indirect) encoding using Compositional Pattern-Producing Network (CPPN) [57] or Bezier splines [58], which are then evolved using genetic algorithms like NeuroEvolution of Augmenting Topologies (NEAT) [59]. Novelty-driven and curiosity-driven algorithms are promising approaches [60, 61, 62].

4.4.3 Better data analysis

Grid traversal of the parameter space (depth-first or breath-first search) is still useful in collecting statistical data, but it needs more reliable algorithms, especially for high-rank metamorphosis-prone species.

All species data collected from automation or crowdsourcing could be stored in a central database for further analysis. Using well-established techniques in related scientific disciplines, the data could be used for dynamical systems analysis (e.g. quasi-period distribution, Lyapunov exponents, transition probabilities matrix), shape analysis (computational anatomy, statistical shape analysis), time-series analysis (cf. in astronomy [63]), and automatic classification (unsupervised or semi-supervised learning).

4.4.4 Variants and generalizations

We could also explore variants and further generalizations of Lenia, for example, higher-dimensional space (especially 3D) [64, 65, 66]; different kinds of grids (e.g. hexagonal, Penrose tiling, irregular mesh) [67, 68, 69]; different structures of kernel (e.g. non-concentric rings); other updating rules (e.g. asynchronous, heterogeneous, stochastic) [70, 71, 72].

4.4.5 Artificial life and artificial intelligence

It has been demonstrated that Lenia shows a few signs of a living system:

- Self-organization, patterns develop well-defined structures
- Self-regulation, patterns maintain dynamical equilibria via oscillation etc.
- Self-direction, patterns move consistently through space
- Adaptability, patterns adapt to changes via plasticity
- Evolvability, patterns evolve via manual operations and potentially genetic algorithms

We should seek whether these are merely superficial resemblances with biological life or are indicators of deeper connections. In the latter case, Lenia could contribute to the endeavors of artificial life in attempting to "understand the essential general properties of living systems by synthesizing life-like behavior in software" [73], or could even add to the debate about the definitions of life as discussed in astrobiology and virology [74, 75]. In the former case, Lenia can still be regarded as a "mental exercise" on how to study a complex system using various methodologies.

Lenia could also be served as a "machine exercise" to provide a substrate or testbed for parallel computing, artificial life and artificial intelligence. The heavy demand in matrix calculation and pattern recognition could act as a benchmark for machine learning algorithms and hardware acceleration; the huge search space of patterns, possibly in higher dimensions, could act as a playground for evolutionary algorithms in the quest of algorithmizing and ultimately understanding open-ended evolution. [76]

5 Online Resources

- Showcase video of Lenia (produced using Python program) at `https://vimeo.com/277328815`
- Source code of Lenia at `http://github.com/Chakazul/Lenia`
- Source code of Primordia at `http://github.com/Chakazul/Primordia`

Acknowledgments

I would like to thank David Ha, Sam Kriegman, Tim Hutton, Kyrre Glette, and Pierre-Yves Oudeyer for valuable discussions, suggestions and insights.

References

[1] M. A. Bedau, J. S. McCaskill, N. H. Packard, S. Rasmussen, C. Adami, D. G. Green, T. Ikegami, K. Kaneko, and T. S. Ray, "Open problems in artificial life," *Artificial Life*, vol. 6, no. 4, pp. 363–376, 2000.

[2] H. Sayama, "Swarm chemistry," *Artificial Life*, vol. 15, no. 1, pp. 105–114, 2009.

[3] T. Schmickl, M. Stefanec, and K. Crailsheim, "How a life-like system emerges from a simple particle motion law," *Scientific Reports*, vol. 6, p. 37969, 2016.

[4] R. P. Munafo, "Stable localized moving patterns in the 2-d gray-scott model." arXiv preprint, 2014.

[5] M. Gardner, "Mathematical games: the fantastic combinations of john conway's new solitaire game "life"," *Scientific American*, vol. 223, no. 4, pp. 120–123, 1970.

[6] S. Wolfram, "Statistical mechanics of cellular automata," *Reviews of Modern Physics*, vol. 55, no. 3, p. 601, 1983.

[7] K. Sims, "Evolving 3d morphology and behavior by competition," *Artificial Life*, vol. 1, no. 4, pp. 353–372, 1994.

[8] N. Cheney, R. MacCurdy, J. Clune, and H. Lipson, "Unshackling evolution: evolving soft robots with multiple materials and a powerful generative encoding," in *Proceedings of the Genetic and Evolutionary Computation Conference*, pp. 167–174, ACM, 2013.

[9] S. Kriegman, N. Cheney, and J. Bongard, "How morphological development can guide evolution," *Scientific Reports*, vol. 8, no. 1, p. 13934, 2018.

[10] M. S. Dodd, D. Papineau, T. Grenne, J. F. Slack, M. Rittner, F. Pirajno, J. O'neil, and C. T. Little, "Evidence for early life in earth's oldest hydrothermal vent precipitates," *Nature*, vol. 543, no. 7643, p. 60, 2017.

[11] D. E. Koshland, "The seven pillars of life," *Science*, vol. 295, no. 5563, pp. 2215–2216, 2002.

[12] C. P. McKay, "What is lifeand how do we search for it in other worlds?," *PLoS Biology*, vol. 2, no. 9, p. e302, 2004.

[13] C. Sagan, "Life," in *Encyclopedia Britannica*, London: William Benton, 1970.

[14] E. Schrdinger, *What is Life?: The Physical Aspect of the Living Cell and Mind and Matter*. Cambridge University Press, 1967.

[15] E. O. Wilson, *Biophilia*. Harvard University Press, 1984.

[16] C. Langton, "Studying artificial life with cellular automata," *Physica D: Nonlinear Phenomena*, vol. 22, no. 1-3, pp. 120–149, 1986.

[17] S. Wolfram, *A New Kind of Science*. Champaign, IL: Wolfram media, 2002.

[18] J. Von Neumann, "The general and logical theory of automata," *Cerebral Mechanisms in Behavior*, vol. 1, no. 41, pp. 1–2, 1951.

[19] S. Ulam, "On some mathematical problems connected with patterns of growth of figures," in *Proceedings of Symposia in Applied Mathematics (Vol. 14)*, pp. 215–224, 1962.

[20] A. Adamatzky, ed., *Game of Life Cellular Automata*. London: Springer, 2010.

[21] ConwayLife.com, "Lifewiki, the wiki for conway's game of life." `http://www.conwaylife.com/wiki/Main_Page`, 2018-12-10. [Online].

[22] P. Rendell, "Turing universality of the game of life," in *Collision-Based Computing*, pp. 513–539, London: Springer, 2002.

[23] B. MacLennan, "Continuous spatial automata," Tech. Rep. CS-90-121, Department of Computer Science, University of Tennessee, Knoxville, 1990.

[24] D. Griffeath, "Self-organization of random cellular automata: four snapshots," in *Probability and Phase Transition*, pp. 49–67, Dordrecht: Springer, 1994.

[25] K. M. Evans, "Larger than life: digital creatures in a family of two-dimensional cellular automata," in *Discrete Mathematics and Theoretical Computer Science Proceedings vol. AA*, pp. 177–192, 2001.

[26] K. M. Evans, "Larger than life: threshold-range scaling of life's coherent structures," *Physica D: Nonlinear Phenomena*, vol. 183, no. 1-2, pp. 45–67, 2003.

[27] M. Pivato, "Reallife: The continuum limit of larger than life cellular automata," *Theoretical Computer Science*, vol. 372, no. 1, pp. 46–68, 2007.

[28] S. Rafler, "Generalization of conway's "game of life" to a continuous domain-smoothlife." arXiv preprint, 2011.

[29] R. P. Munafo, "Catalog of patterns at f=0.0620, k=0.0609." `http://mrob.com/pub/comp/xmorphia/catalog.html`, 2009. [Online].

[30] H. Sayama, "Swarm chemistry homepage — sample recipes." `http://bingweb.binghamton.edu/~sayama/SwarmChemistry/`, 2018-07-29. [Online].

[31] T. J. Hutton, "Smoothlifel glider closeup." `https://www.youtube.com/watch?v=IJO-DETelOM`, 2012-10-10. [Video].

[32] B. Berger, "Big wobbly glider in smoothlife," 2017-03-28. [Video].

[33] W. Kahan, "Lecture notes on the status of ieee standard 754 for binary floating-point arithmetic." `http://http.cs.berkeley.edu/~wkahan/ieee754status/ieee754.ps`, 1997-10-01. [Online].

[34] J. W. Cooley and J. W. Tukey, "An algorithm for the machine calculation of complex fourier series," *Mathematics of Computation*, vol. 19, no. 90, pp. 297–301, 1965.

[35] H. Takagi, "Interactive evolutionary computation: Fusion of the capabilities of ec optimization and human evaluation," *Proceedings of the IEEE*, vol. 89, no. 9, pp. 1275–1296, 2001.

[36] M. K. Hu, "Visual pattern recognition by moment invariants," *IRE Transactions on Information Theory*, vol. 8, no. 2, pp. 179–187, 1962.

[37] J. Flusser, "Moment invariants in image analysis," *In Proceedings of World Academy of Science, Engineering and Technology*, vol. 11, no. 2, pp. 196–201, 2006.

[38] C. Linnaeus, *Systema naturae per regna tria naturae, secundum classes, ordines, genera, species, cum characteribus, differentiis, synonymis, locis.* Stockholm: Impensis Direct, Laurentii Salvii, 10th ed., 1758.

[39] T. Jansen, "Strandbeests," *Architectural Design*, vol. 78, no. 4, pp. 22–27, 2008.

[40] A. Ilachinski, *Cellular Automata: a Discrete Universe.* World Scientific Publishing Company, 2001.

[41] M. Cook, "Universality in elementary cellular automata," *Complex Systems*, vol. 15, no. 1, pp. 1–40, 2004.

[42] S. Wolfram, "Computation theory of cellular automata," *Communications in Mathematical Physics*, vol. 96, no. 1, pp. 15–57, 1984.

[43] C. R. Marshall, "Explaining the cambrian "explosion" of animals," *Annual Review of Earth and Planetary Sciences*, vol. 34, pp. 355–384, 2006.

[44] E. H. P. Haeckel, *Kunstformen der Natur.* Leipzing und Wien, 1904.

[45] K. Porter, "Cil:11397, myotis lucifugus." `http://www.cellimagelibrary.org/images/11397`, 2011. [Online].

[46] R. L. Mayden, "A hierarchy of species concepts: the denouement in the saga of the species problem," in *Species: The Units of Biodiversity* (M. F. Claridge *et al.*, eds.), p. 381424, Springer, 1997.

[47] C. Darwin, *On the Origin of Species.* London: John Murray, 1859.

[48] P. H. Sneath and R. R. Sokal, *Numerical Taxonomy, The Principles and Practice of Numerical Classification.* San Francisco: Freeman, 1973.

[49] J. Mallet, "A species definition for the modern synthesis," *Trends in Ecology & Evolution*, vol. 10, no. 7, pp. 294–299, 1995.

[50] E. Mayr, *Systematics and the Origin of Species, from the Viewpoint of a Zoologist*. Cambridge: Harvard University Press, 1942.

[51] G. G. Simpson, "The species concept," *Evolution*, vol. 5, no. 4, pp. 285–298, 1951.

[52] W. Hennig, *Phylogenetic Systematics*. Urbana: University of Illinois Press, 1966.

[53] L. Van Valen, "Ecological species, multispecies, and oaks," *Taxon*, vol. 25, pp. 233–239, 1976.

[54] J. Secretan, N. Beato, D. Ambrosio, D. B., A. Rodriguez, A. Campbell, and K. O. Stanley, "Picbreeder: evolving pictures collaboratively online," in *Proceedings of the SIGCHI Conference on Human Factors in Computing Systems*, pp. 1759–1768, ACM, 2008.

[55] J. Simon, "Ganbreeder." `https://github.com/joel-simon/ganbreeder`, 2018-12-18. [Code].

[56] D. Ha, "Reinforcement learning for improving agent design." arXiv preprint, 2018.

[57] K. O. Stanley, "Compositional pattern producing networks: A novel abstraction of development," *Genetic Programming and Evolvable Machines*, vol. 8, no. 2, pp. 131–162, 2007.

[58] J. Collins, W. Geles, D. Howard, and F. Maire, "Towards the targeted environment-specific evolution of robot components," in *Proceedings of the Genetic and Evolutionary Computation Conference*, pp. 61–68, ACM, 2018.

[59] K. O. Stanley and R. Miikkulainen, "Evolving neural networks through augmenting topologies," *Evolutionary Computation*, vol. 10, no. 2, pp. 99–127, 2002.

[60] J. Lehman and K. O. Stanley, "Abandoning objectives: Evolution through the search for novelty alone," *Evolutionary Computation*, vol. 19, no. 2, pp. 189–223, 2011.

[61] J. K. Pugh, L. B. Soros, and K. O. Stanley, "Quality diversity: A new frontier for evolutionary computation," *Frontiers in Robotics and AI*, vol. 3, p. 40, 2016.

[62] A. Baranes and P. Y. Oudeyer, "Active learning of inverse models with intrinsically motivated goal exploration in robots," *Robotics and Autonomous Systems*, vol. 61, no. 1, pp. 49–73, 2013.

[63] S. Vaughan, "Random time series in astronomy," *Philosophical Transactions of the Royal Society A: Mathematical, Physical & Engineering Sciences*, vol. 371, no. 1984, p. 20110549, 2012.

[64] C. Bays, "Candidates for the game of life in three dimensions," *Complex Systems*, vol. 1, no. 3, pp. 373–400, 1987.

[65] K. Imai, Y. Masamori, C. Iwamoto, and K. Morita, "On designing gliders in three-dimensional larger than life cellular automata," in *Natural Computing*, pp. 184–190, Tokyo: Springer, 2010.

[66] T. J. Hutton, "A 3d glider in the u-skate world (reaction-diffusion)." `https://www.youtube.com/watch?v=WYZVffOaRgA`, 2012. [Video].

[67] A. Adamatzky, A. Wuensche, and B. D. L. Costello, "Glider-based computing in reaction-diffusion hexagonal cellular automata," *Chaos, Solitons & Fractals*, vol. 27, no. 2, pp. 287–295, 2006.

[68] A. P. Goucher, "Gliders in cellular automata on penrose tilings," *Journal of Cellular Automata*, vol. 7, no. 5-6, pp. 385–392, 2012.

[69] B. Bochenek and K. Tajs-Zieliska, "Gotica - generation of optimal topologies by irregular cellular automata," *Structural and Multidisciplinary Optimization*, vol. 55, no. 6, pp. 1989–2001, 2017.

[70] N. Fates, "A guided tour of asynchronous cellular automata," in *International Workshop on Cellular Automata and Discrete Complex Systems*, (Berlin, Heidelberg), pp. 15–30, Springer, 2013.

[71] C. Ryan, J. Fitzgerald, T. Kowaliw, R. Doursat, S. Carrignon, and D. Medernach, "Evolution of heterogeneous cellular automata in fluctuating environments," in *Proceedings of the European Conference on Artificial Life 13*, pp. 216–223, 2016.

[72] P. Y. Louis and F. R. Nardi, eds., *Probabilistic Cellular Automata: Theory, Applications and Future Perspectives*. Springer, 2018.

[73] M. A. Bedau, "Artificial life: organization, adaptation and complexity from the bottom up," *Trends in Cognitive Sciences*, vol. 7, no. 11, pp. 505–512, 2003.

[74] S. A. Benner, "Defining life," *Astrobiology*, vol. 10, no. 10, pp. 1021–1030, 2010.

[75] P. Forterre, "Defining life: the virus viewpoint," *Origins of Life and Evolution of Biospheres*, vol. 40, no. 2, pp. 151–160, 2010.

[76] T. Taylor, M. Bedau, A. Channon, D. Ackley, W. Banzhaf, G. Beslon, E. Dolson, T. Froese, S. Hickinbotham, T. Ikegami, and B. McMullin, "Open-ended evolution: perspectives from the oee workshop in york," *Artificial Life*, vol. 22, no. 3, pp. 408–423, 2016.

[77] H. Sayama, "Seeking open-ended evolution in swarm chemistry," in *Proceedings of the Third IEEE Symposium on Artificial Life*, pp. 186–193, IEEE, 2011.

[78] H. Sayama, "Seeking open-ended evolution in swarm chemistry ii: Analyzing long-term dynamics via automated object harvesting," in *Proceedings of the 2018 Conference on Artificial Life*, pp. 59–66, 2018.

A Tree of Artificial Life

The notion of "life", here interpreted as self-organizing autonomous entities in a broader sense, may include biological life, artificial life, and other possibilities like extraterrestrial life:

Vitae	
Tree Biota	Biological life
Tree Artificialia	Artificial life
Tree Xenobiota (?)	Extraterrestrial life (undiscovered)

The biological *tree of life*, except the uncertain situation of viruses [75], is widely accepted as:

Biota	
Superdomain Acytota	
Domain Vira (?)	
Superdomain Cytota	
Domain Bacteria, Archaea	
Domain Eukaryota	
Kingdom Protista, Plantae, Fungi, Animalia	

We propose the following *tree of artificial life*, based on lifeforms from Lenia and other models:

Artificialia	
Domain Synthetica	"Wet" biochemical synthetic life
Domain Mechanica	"Hard" mechanical or robotic life, e.g. [39]
Domain Simulata	"Soft" computer simulated life
Kingdom Sims	Evolved virtual creatures, e.g. [7, 8, 9]
Kingdom Greges	Particle swarm solitons, e.g. [77, 78, 30, 3]
Kingdom Turing	Reaction-diffusion solitons, e.g. [29, 4, 66]
Kingdom Automata	Cellular automata patterns
Phylum Discreta	Non-scalable, e.g. [20, 21]
Phylum Lenia	Scalable, e.g. [25, 28]

The current taxonomy of Lenia, according to the definitions of taxonomical ranks ("Taxonomy" section), is:

Phylum Lenia	
Subphylum Stereolenia	Three-dimensional (undiscovered)

Subphylum Planolenia Two-dimensional
- Class Exokernel
  - Order Orbiformes
    - Family Orbidae
  - Order Scutiformes
    - Family Scutidae, Pterifera, Helicidae, Circidae
- Class Mesokernel
  - Order Echiniformes
    - Family Echinidae, Geminidae, Ctenidae, Uridae
- Class Endokernel
  - Order Kroniformes
    - Family Kronidae, Quadridae, Volvidae
  - Order Radiiformes
    - Family Dentidae, Radiidae, Bullidae, Lapillidae, Folidae
  - Order Amoebiformes
    - Family Amoebidae

B Lenia Taxonomy

The followings are the proposed three Lenia classes (Figure 10).

- Class Exokernel are lifeforms that have strong outer kernels rings.
- Class Mesokernel are lifeforms that have kernel rings with similar peak heights.
- Class Endokernel are lifeforms that have strong inner kernels rings.

The followings are the proposed eighteen Lenia families (Figure 8; also Figure 1, 11, 12).

Class Exokernel
Order Orbiformes

O — Orbidae "disk bugs" are composed of halved circular disks (orb), including the singular *Orbium* and *Gyrorbium*, long-chain textsftextsfParorbinae and Synorbinae series. Orbidae are special in Lenia being the fastest moving, rank-1 only, and free from the upper state bound ($\mathbf{A}^t < 1$).

Order Scutiformes

S — Scutidae "shield bugs" are composed of thick circular disks (scutum), including singular *Scutium*, diploid *Pyroscutim*, and long-chain Megaloscutinae series.

P — Pterifera "winged bugs" are composed of wings (pteron) and sacs (vacuole), including singular *Gyropteron*, diploid *Synptera* and *Paraptera*, and long-chain Vacuopterinae series.

H — Helicidae "helix bugs" are rotating versions of Pterifera, including long-chain Perissohelicinae and Artiohelicinae series with odd and even number of vacuoles.

C — Circidae "circle bugs" are single or multiple concentric rings.

Class Mesokernel
Order Echiniformes

E — Echinidae "spiny bugs" is a "waste-bin taxon" with thorny or wavy species.

G — Geminidae "twin bugs" have compartments with heavy lamination, including versatile twin-compartment Diplogemininae and long-chain Polygermininae series.

Ct — Ctenidae "comb bugs" resemble Pterifera but have parallel narrow stripes between wings.

U — Uridae "tail bugs" are large lifeforms with tails of various lengths.

Class Endokernel
Order Kroniformes

K — Kronidae "crown bugs" are complex versions of Scutidae and Pterifera, including singular *Kronium* and deviations like *Argentokronium* and *Aurokronium*, and long-chain Vacuokroninae series.

Q — Quadridae "square bugs" includes versatile *Quadrium* composed of 4×4 square grid of masses.

V — Volvidae "twist bugs" are possibly complex versions of Helicidae.

Order Radiiformes

D — Dentidae "tooth bugs" are rotating species with gear-like units.

R — Radiidae "radial bugs" are regular or star polygons, including triangular Trigonium, cross-like *Crucium*, star-like *Asterium*, and snowflake-like *Nivium*.

B — Bullidae "bubble bugs" are bilateral species consist of an inner ring and an outer bubbled layer.

L — Lapillidae "gem bugs" are small rings distributed around a circle.

F — Folidae "petal bugs" are stationary, thick, radial species with petal-like units.

Order Amoebiformes

A — Amoebidae "amoeba bugs" are volatile species without well-defined shape or behavior.